

94°C for 30 s, annealing at 65°C for 2 min, extension at 72°C for 3 min with a final incubation at 72°C for 10 min. The lengths of the PCR products were determined with an ABI 310 Genetic Analyser and computer software, Genescan and Sequencing Analysis (Perkin-Elmer Biosystems). Sequences of seven alleles of this polymorphism were as follows: allele 1 (160 bp), t(gt)5ac(gt)5ac(gt)11ggcaga(g)6; allele 2 (158 bp), t(gt)5ac (gt)5ac(gt)10ggcaga(g)6; allele 3 (156 bp), t(gt)5ac(gt)5ac(gt)9ggcaga(g)6; allele 4 (144 bp), t(gt)5ac(gt)9ggcaga(g)6; allele 5 (156 bp), t(gt)4ac(gt) 5ac(gt)10ggcaga(g)6; allele 6 (157 bp), t(gt)5ac(gt)5ac(gt)4at(gt)4ggcaga(g)7; allele 7 (160 bp), t(gt)5ac(gt)5at(gt)11ggcaga(g)6. Only alleles 2, 3, and 7 are observed in Japanese (23). The correspondence between the length and the sequence of each PCR product has been confirmed using PCR cycle sequencing by Kojima et al. (23).

### HLA typing

A subset of patients ( $n=54$ ) were genotyped for HLA-DQA1, HLA-DQB1, and HLA-DRB1. Alleles were determined by the PCR-restriction fragment length polymorphism method (25). The most probable HLA-DR and HLA-DQ haplotypes were deduced from known linkage disequilibria (26).

### Statistical analysis

Genotype and allele frequencies were calculated by direct counting. Allele frequencies were initially compared between the disease group and the healthy controls with a  $\chi^2$  test, if applicable, using a  $3 \times 2$  contingency table. Each allele was then analyzed using a  $2 \times 2$  contingency table with a  $\chi^2$  test or a Fisher's exact probability test.  $P$  was corrected by the number of alleles ( $n=3$ ) observed in the Japanese population (Table 1). In analyzing *SLC11A1* polymorphism in terms of *HLA* genotype,  $P$  was corrected 3 times 30, the number of HLA DR-DQ haplotypes observed.  $P$ - or  $P_c$  (corrected  $P$ )-values  $<0.05$  were considered to be statistically significant. The strength of association was estimated by the odds ratio.

## Results

In all Japanese subjects examined, three alleles, alleles 2, 3, and 7, were identified in the *SLC11A1*-promoter region, while alleles 1, 4, 5, and 6 were not. These results were consistent with those of the previous studies on Japanese subjects (23). Gender and age did not affect allele frequencies of this polymorphism (data not shown). Allele 7 was noted to be positively associated with type 1 diabetes ( $P=0.03$  and  $P_c=0.042$ , with a  $\chi^2$  test using  $2 \times 2$  and  $3 \times 2$  contingency tables, respectively) (Table 1). The frequency of alleles 2 and 3 did not differ between the type 1 diabetic subjects and controls with a Bonferroni multiple adjustment using a  $2 \times 2$  contingency table (Table 1).

Because the *HLA* gene (*IDDM1*) exerts the greatest influence on the susceptibility to type 1 diabetes, association of the *SLC11A1* polymorphism with diabetes was analyzed in terms of the *IDDM1* genotype. A subset of the subjects with diabetes ( $n=54$ ) were analyzed for *HLA* class II genotype, and this subpopulation was employed for further analysis. The *HLA* allele frequencies in this subpopulation were similar to those of a recent Japanese report (27) (data not shown). In addition, the *SLC11A1* allele frequencies of this subpopulation (allele 2, 9.4%; allele 3, 80.2%; allele 7, 10.4%) were very similar to those of whole type 1 diabetic population (allele 2, 11.6%; allele 3, 78.9%; allele 7, 9.5%). This subpopulation was stratified according to the presence of susceptibility, neutral, and protective alleles for *IDDM1*. The diabetic subjects with high-risk *HLA* haplotypes, DR4-DQ4/X ( $n=16$ , X does not contain DR9-DQ9 or protective alleles), DR9-DQ9/Y ( $n=16$ , Y does not contain DR4-DQ4 or protective alleles), or DR4-DQ4/DR9-DQ9 ( $n=5$ ), did not show a significant difference in the allele distribution of *SLC11A1*, as compared with the controls. On the contrary, the rest ( $n=17$ ) of the diabetic subjects with at least one protective allele, DRB1\*0601, in combination with any haplotype, and those without any susceptibility haplotypes had a much higher allele 7 frequency (23.5%) than the controls (4.5%) ( $P_c=0.0042$ , Fisher's exact probability test) (Table 2).

Allele frequencies of polymorphisms in the promoter region of *SLC11A1*

Allele	Subject	Allele frequency (%)	Odds ratio	95% CI	$P_c$ by $2 \times 2 \chi^2$ test	$P$ by $2 \times 3 \chi^2$ test
2	Type 1 diabetes ( $n=95$ )	11.6	0.72	0.43–1.2	0.62	
	Control ( $n=224$ )	15.4				
3	Type 1 diabetes ( $n=95$ )	78.9	0.93	0.61–1.4	2.2	
	Control ( $n=224$ )	80.1				
7	Type 1 diabetes ( $n=95$ )	9.47	2.2	1.2–4.3	0.042	0.030
	Control ( $n=224$ )	4.46				

Table 1

Allele frequencies of the *SLC11A1*-promoter polymorphisms in the HLA-genotyped subjects with type 1 diabetes mellitus

Allele	Subject	Allele frequency (%)	Odds ratio	95% CI	P <sup>a</sup>
2	HLA-genotyped patients (n = 54)	9.43	0.57	0.29–1.1	0.33
	DR4-DQ4/X (n = 16)	10.7	0.57	0.17–1.9	24 <sup>b</sup>
	DR9-DQ9/Y (n = 16)	10.7	0.57	0.17–1.9	24 <sup>b</sup>
	DR4-DQ4/DR9-DQ9 (n = 5)	20.0	1.37	0.29–6.6	42 <sup>b</sup>
	Any/P or N/N (n = 17)	5.88	0.34	0.090–1.4	8.7 <sup>b</sup>
	Control (n = 224)	15.4			
3	HLA-genotyped patients (n = 54)	80.2	1.0	0.59–1.7	3.0
	DR4-DQ4/X (n = 16)	87.5	1.7	0.65–3.1	33 <sup>b</sup>
	DR9-DQ9/Y (n = 16)	81.3	1.1	0.43–2.7	78 <sup>b</sup>
	DR4-DQ4/DR9-DQ9 (n = 5)	80.0	1.0	0.21–4.8	63 <sup>b</sup>
	Any/P or N/N (n = 17)	70.6	0.6	0.28–1.3	78 <sup>b</sup>
	Control (n = 224)	80.1			
7	HLA-genotyped patients (n = 54)	10.4	2.5	1.2–23	0.017
	DR4-DQ4/X (n = 16)	3.13	0.69	0.090–5.3	54 <sup>b</sup>
	DR9-DQ9/Y (n = 16)	10.7	2.2	0.64–7.7	17 <sup>b</sup>
	DR4-DQ4/DR9-DQ9 (n = 5)	0.00	0.0		57 <sup>b</sup>
	Any/P or N/N (n = 17)	23.5	6.6	2.9–15	0.0042 <sup>b</sup>
	Control (n = 224)	4.46			

<sup>a</sup>Fischer's exact test was used, when  $\chi^2$  test was not applicable.

<sup>b</sup>P was corrected 3 times 30, the number of *SLC11A1* alleles and HLA DR-DQ haplotypes observed, respectively.

N, neutral alleles; P, protective alleles; X, not containing DR9-DQ9 or protective alleles; Y, not containing DR4-DQ4 or protective alleles.

Table 2

## Discussion

To our knowledge, this is the first report to show an association of type 1 diabetes with allele 7 of the *SLC11A1*-promoter polymorphism. Kojima et al. (23) recently identified allele 7 in Japanese, which has the same length with, but different sequence from, allele 1 and also showed the absence of allele 1 in Japanese. The *SLC11A1*-promoter polymorphism in a Japanese population was previously determined only by length, but not by sequences (21, 28, 29). Because alleles 1 and 7 are the same in length but different in sequence, the allele 1 in these reports must be allele 7.

In Caucasians, stronger promoter activity of allele 3 to drive higher *SLC11A1* expression than other alleles leads to the hypothesis that the high expression of *SLC11A1* promoted by allele 3 may produce chronic macrophage hyperactivation, causing autoimmune diseases (14). The activity of allele 7 has not been determined so far, and hence we cannot interpret our present data in functional regards. Similar to allele 1, which reportedly has low promoter activity in Caucasian, allele 7 also has 11 GT repeats. The length is the same and the sequences are basically similar between allele 1 and allele 7. These two alleles, however, possibly are different in their ability to drive

gene expression, because a single-nucleotide substitution in the promoter region of a gene can alter transcriptional efficiency (30–32). Positive association of allele 7 with Crohn's disease, ulcerative colitis (23), and Kawasaki disease (28), in which chronic activation of monocytes/macrophages and consequent high production of monokines play key roles, lead us to surmise that this allele possesses strong activity to drive *SLC11A1* expression. A functional study of this allele is necessary to shed light on the association of allele 7 with type 1 diabetes.

Our present results are not completely in line with a recent report by Bassuny et al. (21) that showed negative association of allele 2 with early-onset type 1 diabetic subjects in Japanese, although the difference did not reach statistical significance. In our study, the frequencies of allele 2, 3, and 7 were 15, 74, and 11%, respectively in early-onset subpopulation (age of onset, <10, n = 120, P = 0.11 by  $\chi^2$  test) and 5.7, 87, and 7.1% respectively in late-onset subpopulation (age of onset, >10, n = 70). In whole type 1 diabetic subjects, allele 2 frequency was significantly lower with a  $\chi^2$  test using a 3 × 2 contingency table, but not with a Bonferroni multiple adjustment using a 2 × 2 contingency table (Table 1). The negative association of allele 2 with type 1 diabetes needs to be validated in Japanese population,

because this would uphold the hypothesis in Caucasians; the lower *SLC11A1* expression level promoted by allele 2 leads to insufficient activation of macrophages, thereby enhancing resistance to autoimmune diseases.

We found allele 7 as a culprit, but Bassuny et al. (21) did not. Control subjects in their report displayed higher allele 7 frequency (8.2%) than ours and other previous reports conducted in an East Asian population. Allele 7 frequency of our control subjects, 4.5% in Sendai, seems more likely as one of those observed in East Asia; 2.2, 3.2, and 4.0 in Tokyo and Osaka (29), Kawasaki (28), and Korea (33), respectively.

It is noteworthy that this polymorphism showed much stronger association with type 1 diabetes in the subpopulation of those lacking one of two diabetes-susceptibility HLA haplotypes and those possessing at least one protective allele. This observation is similar to previous findings on *IDDM13* in Caucasian (17) and Japanese (34) subjects; a stronger association of type 1 diabetes with the *IDDM13*

gene was observed in subjects without the major susceptibility HLA alleles. This may explain why we detected a significant contribution of *SLC11A1* in a case-control study in Japanese. Because Japanese have a lower frequency of strong susceptibility HLA haplotypes than Caucasians, the contribution of *SLC11A1* to type 1 diabetes susceptibility may be easier to detect.

Although it is possible that the *SLC11A1* polymorphism is directly involved in the predisposition to type 1 diabetes, other possibilities including linkage disequilibrium of this polymorphism with a susceptibility gene remain to be elucidated. In proximity to the *SLC11A1* are several genes which has been suggested to be involved in the pathogenesis of this disease, including IL-8 receptor  $\alpha$  and  $\beta$  and caspase 8 genes.

In summary, allele 7 of the *SLC11A1* is an important predisposing factor for type 1 diabetes development especially in the Japanese population. These observations should be examined in other especially Asians ethnic populations.

## References

- Ashton-Rickardt PG, Bandeira A, Delaney JR et al. Evidence for a differential avidity model of T cell selection in the thymus. *Cell* 1994; **76**: 651–63.
- Rocha B, von Boehmer H. Peripheral selection of the T cell repertoire. *Science* 1991; **251**: 1225–31.
- Ucker DS, Meyers J, Obermiller PS. Activation-driven T cell death. II. Quantitative differences alone distinguish stimuli triggering nontransformed T cell proliferation or death. *J Immunol* 1993; **149**: 1583–92.
- Critchfield JM, Racke MK, Zuniga-Pflucker JC et al. T cell deletion in high antigen dose therapy of autoimmune encephalomyelitis. *Science* 1994; **263**: 1139–43.
- Takahashi K, Honeyman MC, Harrison LC. Impaired yield, phenotype, and function of monocyte-derived dendritic cells in humans at risk for insulin-dependent diabetes. *J Immunol* 1998; **161**: 2629–35.
- Yokono K, Kasase Y, Nagata M, Hatamori N, Baba S. Suppression of concanavalin A-induced responses in splenic lymphocytes by activated macrophages in the non-obese diabetic mouse. *Diabetologia* 1989; **32**: 67–73.
- Smerdon RA, Peakman M, Hussain MJ et al. Increase in simultaneous coexpression of naive and memory lymphocyte markers at diagnosis of IDDM. *Diabetes* 1993; **42**: 127–33.
- Serreze DV, Gaskins HR, Leiter EH. Defective activation of T suppressor cell function in nonobese diabetic mice: potential relationship to cytokine deficiencies. *J Immunol* 1993; **150**: 2534–43.
- Milich DR, Jones JE, McLachlan A, Houghten R, Thornton GB, Hughes JL. Distinction between immunogenicity and tolerogenicity among HBcAg T cell determinants. Influence Peptide–MHC Interaction. *J Immunol* 1989; **143**: 3148–56.
- Mamula MJ. The inability to process a self-peptide allows autoreactive T cells to escape tolerance. *J Exp Med* 1993; **17**: 567–71.
- Serreze DV, Leiter EH. Defective activation of T suppressor cell function in nonobese diabetic mice: potential relation to cytokine deficiencies. *J Immunol* 1988; **140**: 3801–7.
- Serreze DV, Leiter EH. Development of diabetogenic T cells from NOD/Lt marrow is blocked when an allo-H-2 haplotype is expressed on cells of hemopoietic origin, but not on thymic epithelium. *J Immunol* 1991; **147**: 1222–9.
- Merriman TR, Todd JA. Genetics of insulin-dependent diabetes: non-major histocompatibility genes. *Horm Metab Res* 1996; **28**: 289–93.
- Searle S, Blackwell JM. Evidence for a functional repeat polymorphism in the promoter of the human *SLC11A1* gene that correlates with autoimmune versus infectious disease susceptibility. *J Med Genet* 1999; **36**: 295–9.
- Copeman JB, Cucca F, Hearne CM et al. Linkage disequilibrium mapping of a type 1 diabetes susceptibility gene (*IDDM7*) to chromosome 2q31–q33. *Nat Genet* 1995; **9**: 80–5.
- Nistico L, Buzzetti R, Pritchard LE et al. The *CTLA-4* gene region of chromosome 2q33 is linked to, and associated with, type 1 diabetes. *Hum Mol Genet* 1996; **5**: 1075–80.
- Morahan G, Huang D, Tait BD, Colman PG, Harrison LC. Markers on distal chromosome 2q linked to insulin-dependent diabetes mellitus. *Science* 1996; **272**: 1811–3.
- Awata T, Kurihara S, Iitaka M et al. Association of *CTLA-4* gene A-G polymorphism (*IDDM12* locus) with acute-onset and insulin-depleted IDDM as well as autoimmune thyroid disease (Graves' disease and Hashimoto's thyroiditis) in the Japanese population. *Diabetes* 1998; **47**: 128–9.
- Iwata I, Nagafuchi S, Nakashima H et al. Association of polymorphism in the *NeuroD/BETA2* gene with type 1 diabetes in the Japanese. *Diabetes* 1999; **48**: 416–9.

20. Hill NJ, Lyons PA, Armitage N, Todd JA, Wicker LS, Peterson LB. NOD Idd5 locus controls insulinitis and diabetes and overlaps the orthologous CTLA4/IDDM12 and SLC11A1 loci in humans. *Diabetes* 2000; **49**: 1744–7.
21. Bassuny WM, Ihara K, Matsuura N et al. Association study of the NRAMP1 gene promoter polymorphism and early-onset type 1 diabetes. *Immunogenetics* 2002; **54**: 282–5.
22. Esposito L, Hill NJ, Pritchard LE et al. Genetic analysis of chromosome 2 in type 1 diabetes: analysis of putative loci IDDM7, IDDM12, and IDDM13 and candidate genes NRAMP1 and IA-2 and the interleukin-1 gene cluster. IMDIAB Group. *Diabetes* 1998; **47**: 1797–9.
23. Kojima Y, Kinouchi K, Takahashi S et al. Inflammatory bowel disease is associated with a novel promoter polymorphism of SLC11A1 gene. *Tissue Antigens* 2001; **58**: 379–84.
24. Bando Y, Ushioji Y, Toya D, Tanaka N, Fujisawa M. Antibodies to glutamic acid decarboxylase (GAD) in non-obese Japanese diabetics without insulin therapy: a comparison of two commercial RIA kits based on recombinant and pig brain GAD. *Diabetes Res Clin Pract* 1998; **41**: 25–33.
25. Bidwell J. DNA-RFLP analysis and genotyping of HLA-DR and DQ antigens. *Immunol Today* 1988; **9**: 18–23.
26. Imahashi T, Akaza T, Kimura A, Tokunaga K, Gojobori T. Allele and haplotype frequencies for HLA and complement loci in various ethnic groups. In: Tsuji K, Aizawa M, Sasazuki T, eds. *HLA 1991: Proceedings of the Eleventh International Histocompatibility Workshop and Conference*. Oxford: Oxford University Press, 1992: 1065–220.
27. Kawabata Y, Ikegami H, Kawaguchi Y et al. Asian-specific HLA haplotypes reveal heterogeneity of the contribution of HLA-DR and -DQ haplotypes to susceptibility to type 1 diabetes. *Diabetes* 2002; **51**: 545–51.
28. Ouchi K, Suzuki Y, Shirakawa T, Kishi F. Polymorphism of SLC11A1 (formerly NRAMP1) gene confers susceptibility to Kawasaki disease. *J Infect Dis* 2003; **187**: 326–9.
29. Gao PS, Fujishima S, Mao XQ et al. Genetic variants of NRAMP1 and active tuberculosis in Japanese populations. International Tuberculosis Genetics Team. *Clin Genet* 2000; **58**: 74–6.
30. Fishman D, Faulds G, Jeffery R et al. The effect of novel polymorphisms in the interleukin-6 (IL-6) gene on IL-6 transcription and plasma IL-6 levels, and an association with systemic-onset juvenile chronic arthritis. *J Clin Invest* 1998; **102**: 1369–76.
31. Li LC, Chui RM, Sasaki M et al. A single nucleotide polymorphism in the E-cadherin gene promoter alters transcriptional activities. *Cancer Res* 2000; **60**: 873–6.
32. Crawley E, Kay R, Sillibourne J, Patel P, Hutchinson I, Woo P. Polymorphic haplotypes of the interleukin-10 5' flanking region determine variable interleukin-10 transcription and are associated with particular phenotypes of juvenile rheumatoid arthritis. *Arthritis Rheum* 1999; **42**: 1101–8.
33. Yang YS, Kim SJ, Kim JW, Koh EM. NRAMP1 gene polymorphisms in patients with rheumatoid arthritis in Koreans *J Korean Med Sci* 2000; **15**: 83–7.
34. Fu J, Ikegami H, Kawaguchi Y et al. Association of distal chromosome 2q with IDDM in Japanese subjects. *Diabetologia* 1998; **41**: 228–32.



## Overexpression of constitutively activated glutamate dehydrogenase induces insulin secretion through enhanced glutamate oxidation

Takatoshi Anno,<sup>1</sup> Shunsuke Uehara,<sup>2</sup> Hideki Katagiri,<sup>3</sup> Yasuharu Ohta,<sup>1</sup> Kohei Ueda,<sup>1</sup> Hiroyuki Mizuguchi,<sup>4</sup> Yoshinori Moriyama,<sup>2</sup> Yoshitomo Oka,<sup>3</sup> and Yukio Tanizawa<sup>1</sup>

<sup>1</sup>Division of Molecular Analysis of Human Disorders, Department of Bio-Signal Analysis, Yamaguchi University Graduate School of Medicine, Ube, Yamaguchi 755-8505; <sup>2</sup>Department of Biochemistry, Faculty of Pharmaceutical Sciences, Okayama University, Okayama 700-8530; <sup>3</sup>Division of Molecular Metabolism and Diabetes, Department of Internal Medicine, Tohoku University Graduate School of Medicine, Sendai 980-8574; and <sup>4</sup>Division of Cellular and Gene Therapy Products, National Institute of Health Sciences, Tokyo 158-8501, Japan

Submitted 25 August 2003; accepted in final form 2 October 2003

Anno, Takatoshi, Shunsuke Uehara, Hideki Katagiri, Yasuharu Ohta, Kohei Ueda, Hiroyuki Mizuguchi, Yoshinori Moriyama, Yoshitomo Oka, and Yukio Tanizawa. Overexpression of constitutively activated glutamate dehydrogenase induces insulin secretion through enhanced glutamate oxidation. *Am J Physiol Endocrinol Metab* 286: E280–E285, 2004. First published October 7, 2003; 10.1152/ajpendo.00380.2003.—Glutamate dehydrogenase (GDH) catalyzes reversible oxidative deamination of L-glutamate to  $\alpha$ -ketoglutarate. Enzyme activity is regulated by several allosteric effectors. Recognition of a new form of hyperinsulinemic hypoglycemia, hyperinsulinism/hyperammonemia (HI/HA) syndrome, which is caused by gain-of-function mutations in GDH, highlighted the importance of GDH in glucose homeostasis. GDH266C is a constitutively activated mutant enzyme we identified in a patient with HI/HA syndrome. By overexpressing GDH266C in MIN6 mouse insulinoma cells, we previously demonstrated unregulated elevation of GDH activity to render the cells responsive to glutamine in insulin secretion. Interestingly, at low glucose concentrations, basal insulin secretion was exaggerated in such cells. Herein, to clarify the role of GDH in the regulation of insulin secretion, we studied cellular glutamate metabolism using MIN6 cells overexpressing GDH266C (MIN6-GDH266C). Glutamine-stimulated insulin secretion was associated with increased glutamine oxidation and decreased intracellular glutamate content. Similarly, at 5 mmol/l glucose without glutamine, glutamine oxidation also increased, and glutamate content decreased with exaggerated insulin secretion. Glucose oxidation was not altered. Insulin secretion profiles from GDH266C-overexpressing isolated rat pancreatic islets were similar to those from MIN6-GDH266C, suggesting observation in MIN6 cells to be relevant in native  $\beta$ -cells. These results demonstrate that, upon activation, GDH oxidizes glutamate to  $\alpha$ -ketoglutarate, thereby stimulating insulin secretion by providing the TCA cycle with a substrate. No evidence was obtained supporting the hypothesis that activated GDH produced glutamate, a recently proposed second messenger of insulin secretion, by the reverse reaction, to stimulate insulin secretion.

hypoglycemia; hyperinsulinism/hyperammonemia syndrome; islet of Langerhans

THE MITOCHONDRIAL MATRIX ENZYME glutamate dehydrogenase (GDH; EC 1.4.1.3) catalyzes reversible oxidative deamination of L-glutamate to  $\alpha$ -ketoglutarate with NAD(P) as a cofactor. The activity of this enzyme is regulated positively and negatively by several allosteric effectors, including amino acids

Address for reprint requests and other correspondence: Y. Tanizawa, Div. of Molecular Analysis of Human Disorders, Dept. of Bio-Signal Analysis, Yamaguchi Univ. Graduate School of Medicine, Minami-Kogushi Ube, Yamaguchi 755-8505, Japan (E-mail: tanizawa@yamaguchi-u.ac.jp).

(leucine, isoleucine, valine, methionine), ADP, and GTP. In pancreatic  $\beta$ -cells, GDH has been suggested to be involved in the regulation of insulin secretion, especially leucine-stimulated insulin secretion (18, 19). The importance of GDH in glucose homeostasis is also evident from recent findings that gain-of-function mutations in the *GLUD1* gene, which encodes GDH, cause hyperinsulinism/hyperammonemia (HI/HA) syndrome (9, 20, 21, 22, 25, 29).

Previously, we identified a *GLUD1* gene mutation, Y266C, in a patient with HI/HA syndrome (22). The activity of the mutant GDH (GDH266C) was constitutively elevated, and allosteric regulations by ADP and GTP were severely impaired. Using GDH266C as a tool, we showed unregulated elevation of GDH activity in MIN6 insulinoma cells to render the cells responsive to glutamine. Glutamine stimulated insulin secretion from these cells in the absence of leucine, an allosteric activator of GDH. We also demonstrated insulin secretion to be exaggerated in these cells at low glucose concentrations (22). Glutamine alone, to which the plasma membrane is permeable and which is readily converted to glutamate intracellularly, does not normally stimulate insulin release. However, it remarkably stimulates insulin secretion in the presence of leucine. It is generally accepted that, in pancreatic  $\beta$ -cells, activation of GDH by allosteric effectors, such as leucine, enhances glutamate oxidation and increases ATP production by providing the tricarboxylic acid (TCA) cycle with  $\alpha$ -ketoglutarate and thereby stimulates insulin secretion (18, 19). Physiologically, GDH is also suggested to play an important role in basal insulin secretion (2, 5). Our previous observations (22) in MIN6 cells are in good agreement with this theory.

On the other hand, mitochondrially derived glutamate was suggested to be a second messenger in glucose-stimulated insulin secretion, acting directly on insulin-secretory granules (4, 11, 17). This theory assumes reverse flux through GDH in the direction of glutamate formation, and glutamate-induced insulin secretion was suggested to correlate with the level of GDH expression (4, 10). However, this hypothesis is controversial and has been contradicted by other studies (2, 8). Furthermore, it was recently demonstrated that cellular glutamate content did not correlate with the amplification of insulin secretion (1, 7). Most previous studies have investigated the role of GDH in insulin secretion by activating intracellular

The costs of publication of this article were defrayed in part by the payment of page charges. The article must therefore be hereby marked "advertisement" in accordance with 18 U.S.C. Section 1734 solely to indicate this fact.

GDH with allosteric activators such as leucine or  $\beta$ -aminobicyclo[2.2.1]heptane-2-carboxylic acid. Identification of constitutively activated mutant GDH (GHD266C) enabled us to study the effects of elevated intracellular GDH activity on insulin secretion more directly by introducing the mutant enzyme into cells. Our present study was designed to investigate directly the correlations among insulin secretion, GDH activity, and cellular glutamate metabolism. We also studied changes in insulin secretion profiles caused by unregulated elevation of GDH activity in native  $\beta$ -cells to confirm the physiological relevance of our findings in MIN6 cells. Our results further clarify the role of GDH in the regulation of insulin secretion and provide insights into the pathophysiology of the HI/HA syndrome.

#### MATERIALS AND METHODS

**Analysis of glutamine and glucose oxidation.** MIN6 cells overexpressing the mutant GDH via retrovirus-mediated gene transfer (MIN6-GDH266C) and control lacZ-overexpressing cells (MIN6-lacZ) were used for these experiments (22). Cells were seeded onto a 6-cm dish at a concentration of  $4.0 \times 10^6$  cells/dish and cultured in DMEM-MIN6 medium (Sigma, St. Louis, MO) containing 25 mmol/l glucose supplemented with 15% heat-inactivated fetal calf serum, 72  $\mu$ mol/l  $\beta$ -mercaptoethanol, 50 U/ml penicillin G, and 50  $\mu$ g/ml streptomycin. Sixty hours later, glutamine or glucose oxidation was assayed. After a 30-min preincubation in HEPES-balanced Krebs-Ringer bicarbonate buffer (HB-KRBB; in mmol/l: 10 HEPES, 120 NaCl, 4.7 KCl, 1.2 MgSO<sub>4</sub>, 1.2 KH<sub>2</sub>PO<sub>4</sub>, 20 NaHCO<sub>3</sub>, and 2 CaCl<sub>2</sub>, pH 7.4) containing 0.5% BSA and 5 mmol/l glucose, radioactive L-[U-<sup>14</sup>C]glutamine (0.05  $\mu$ Ci, 261 Ci/mol; Amersham, Buckinghamshire, UK) or radioactive D-[6-<sup>14</sup>C]glucose [0.04  $\mu$ Ci (for 5 mmol/l glucose) or 0.20  $\mu$ Ci (for 25 mmol/l glucose), 58.0 Ci/mol; Amersham] was added to 4 ml of fresh HB-KRBB containing 0.5% BSA and various concentrations of glutamine or glucose. Then, MIN6-GDH266C or MIN6-lacZ cells in the culture dishes were placed immediately in sealed glass containers (7 cm diameter  $\times$  10 cm height) filled with 100% oxygen and incubated for 30 min (glutamine oxidation) or 1 h (glucose oxidation) at 37°C. At completion of the incubations, 0.5 ml of 10% HClO<sub>4</sub> was added to the medium by means of a long 21-gauge needle through rubber stoppers on the top of the container, allowing CO<sub>2</sub> gas (containing radioactive [<sup>14</sup>C]CO<sub>2</sub>) to evaporate and be trapped in 2 ml of 10% KOH solution in a small glass cup suspended above the medium in a sealed glass container. The glass containers were incubated for another 30 min, and the KOH solution was then transferred to scintillation vials containing 10 ml of Aquasol-2 (PerkinElmer, Boston, MA), and radioactivity was measured with a liquid scintillation counter. With this system,  $90.7 \pm 1.2\%$  (mean  $\pm$  SE;  $n = 3$ ) of CO<sub>2</sub> gas, evaporating from the medium containing 0.5  $\mu$ Ci NaH[<sup>14</sup>C]O<sub>3</sub> (Amersham), was trapped in KOH solution.

**Measurement of intracellular glutamate content.** MIN6-GDH266C and control MIN6-lacZ cells were seeded onto six-well plates at a concentration of  $1.8 \times 10^6$  cells/well and cultured in DMEM-MIN6 medium. Sixty hours later, glutamate contents were assayed. After a 30-min preincubation in HB-KRBB containing 0.5% BSA and 5 mmol/l glucose, the preincubation buffer was replaced with fresh HB-KRBB containing 0.5% BSA and various concentrations of glutamine or glucose, and the cells were incubated for an additional hour at 37°C. At the end of the incubation, the cells were quickly washed on ice with ice-cold HB-KRBB, and 1 ml of 6% perchloric acid was immediately added. The cells were then collected and sonicated on ice. After centrifugation at 15,000 rpm for 5 min, the supernatant (800  $\mu$ l) was collected, and 275  $\mu$ l of 30% KOH were added. White precipitates were removed by brief centrifugation, and the supernatant was kept at  $-80^\circ\text{C}$  for the glutamate measurement. Cells in one of the

wells were homogenized in PBS and used for protein determination. The amount of glutamate was determined, using an aliquot of the cell extract, by high-performance liquid chromatography with precolumn *o*-phthalaldehyde derivatization, separation on a reverse-phase Resolve C18 column (3.9  $\times$  150 mm; Waters, Toronto, ON, Canada), and fluorescence detection (3, 27, 28).

**Construction of recombinant adenoviruses and adenovirus-mediated gene transfer.** pcDNA3-hGDH-WT and pcDNA3-hGDH266C (22) were digested with *NotI* and *SnaBI*. The fragments containing GDH cDNA were then ligated into *NotI*- and *SnaBI*-digested pShuttle vectors (14, 15). The resultant plasmids, pShuttle-hGDH-WT and pShuttle-hGDH266C, were then digested with *I-CeuI*/*PI-SceI* and ligated into *I-CeuI*/*PI-SceI*-digested pAdHM4 (14, 15) to produce pAd-hGDH-WT and pAd-hGDH266C. They were then linearized with *PacI* and transfected into 293 human embryonic kidney cells with FuGENE6 (Roche Diagnostics, Mannheim, Germany) according to the manufacturer's instructions. Recombinant adenoviruses expressing GDH-WT and GDH266C (Ad-hGDH-WT and Ad-hGDH266C) were thus obtained and amplified via infection of 293 cells. As a control, we also constructed an adenoviral vector to express enhanced green fluorescent protein (eGFP; Ad-eGFP). Titers of the recombinant adenovirus stocks were  $6.0 \times 10^7$  (Ad-hGDH-WT),  $5.5 \times 10^7$  (Ad-hGDH266C), and  $9.5 \times 10^7$  plaque-forming units (pfu)/ml (Ad-eGFP).

Pancreatic islets were isolated by collagenase digestion as described previously (6, 24). Isolated islets were cultured on a 60-mm tissue culture dish with RPMI 1640 medium containing 11 mmol/l glucose supplemented with 10% fetal calf serum, 50 U/ml penicillin, and 50  $\mu$ g/ml streptomycin (RPMI-islet) and maintained at 37°C in humidified 5% CO<sub>2</sub>-95% air. Twenty-four to thirty-six hours after isolation, groups of 50–100 islets were incubated with the recombinant adenoviruses at a multiplicity of infection (moi) of  $\sim 4 \times 10^5$  pfu/islet. After a 1-h incubation with the adenovirus at 37°C, the medium was removed, and the islets were washed once with phosphate-buffered saline (PBS). The islets were then further incubated on a 60-mm tissue culture dish with RPMI-islet medium. Experiments were performed 24 h after infection.

**GDH enzyme assay.** COS-7 cells and isolated pancreatic islets were infected with recombinant adenoviruses at an moi of  $\sim 10$  pfu/cell or  $4 \times 10^5$  pfu/islet, respectively. Forty-eight (COS-7) or 24 (islets) h after the infection, cells were washed, suspended in PBS, and sonicated to prepare crude cell extract. GDH activity was measured by the oxidation of NADH ( $\epsilon_{340 \text{ nm}} = 6.22 \times 10^3 \text{ mol}^{-1} \cdot \text{l}^{-1} \cdot \text{cm}^{-1}$ ), as described previously (26), with a Beckman Coulter (Fullerton, CA) Spectrophotometer model DU-640 at 25°C. The assay solution (1 ml) consisted of 10 mmol/l Tris-acetate (pH 8.0), 10  $\mu$ mol/l EDTA, 100  $\mu$ mol/l NADH, 50 mmol/l NH<sub>4</sub>Cl, and 5 mmol/l  $\alpha$ -ketoglutarate. ADP, GTP, or leucine was added to the solution at various concentrations. The reaction was started by adding appropriate amounts (30–50  $\mu$ l) of cell extracts, and the decrease in absorbance at 340 nm was measured for 5 min. During this incubation period, the reaction was linear, and there was no indication of GTP hydrolysis, substrate depletion, or product saturation. The activity was determined in duplicate for each sample.

**Analysis of insulin secretion.** Groups of 10–30 islets overexpressing the mutant GDH (Islets-GDH266C) and eGFP (Islets-eGFP) via adenovirus-mediated gene transfer were used for each assay. Insulin secretion was examined by the static incubation method (23, 24). In brief, after a 30-min preincubation in HB-KRBB supplemented with 0.5% BSA and 5 mmol/l glucose, the preincubation buffer was replaced with fresh HB-KRBB containing 0.5% BSA and various concentrations of glutamine or glucose. After an additional 30-min incubation at 37°C, the buffer was collected, and immunoreactive insulin was measured by radioimmunoassay using rat insulin (Linco Research, St. Charles, MO) as a standard. The amounts of secreted insulin were corrected by the amounts of cell protein in each well.

## RESULTS

**Glutamine and glucose metabolism in MIN6-GDH266C cells.** We investigated the metabolic changes associated with elevated GDH activity. We used MIN6-GDH266C as a model. When the cells were incubated in the presence of glutamine (1 mmol/l) with a tracer of L-[U-<sup>14</sup>C]glutamine, glutamine oxidation was increased in MIN6-GDH266C compared with control MIN6-lacZ ( $P < 0.02$ , unpaired *t*-test; Fig. 1A). In agreement with the enhanced glutamine oxidation, intracellular glutamate content in MIN6-GDH266C was lower than that in MIN6-lacZ ( $P < 0.01$  at 1.0 mmol/l; Fig. 1B).

At low glucose concentrations (without exogenous glutamine), insulin secretion was augmented in MIN6-GDH266C (22). We then studied metabolic changes under these condi-

tions. Glucose oxidation did not differ between MIN6-GDH266C and MIN6-lacZ [ $4.0 \pm 0.7$  vs.  $4.0 \pm 0.9$  pmol/ $\mu$ g protein at 5 mmol/l glucose ( $P > 0.9$ ; Fig. 2A) and  $7.9 \pm 2.0$  vs.  $6.8 \pm 1.9$  pmol/ $\mu$ g protein at 25 mmol/l glucose ( $P > 0.6$ ; unpaired *t*-test)]. Cellular glutamine oxidation, however, was significantly enhanced in MIN6-GDH266C [ $46.7 \pm 1.2$  vs.  $27.2 \pm 1.6$  pmol/ $\mu$ g protein at 5 mmol/l glucose ( $P < 0.001$ ; Fig. 2B) and  $31.7 \pm 4.1$  vs.  $16.4 \pm 2.0$  pmol/ $\mu$ g protein at 25 mmol/l glucose ( $P < 0.03$ ; unpaired *t*-test)]. The corresponding intracellular glutamate content was decreased in MIN6-GDH266C compared with that in MIN6-lacZ [ $10.3 \pm 2.0$  vs.  $25.4 \pm 2.3$  pmol/ $\mu$ g protein at 5 mmol/l glucose ( $P < 0.002$ ; Fig. 2C) and  $14.2 \pm 1.3$  vs.  $36.6 \pm 2.1$  pmol/ $\mu$ g protein at 25 mmol/l glucose ( $P < 0.001$ ; unpaired *t*-test)]. These results indicate that elevated GDH activity enhances glutamine oxidation and probably increases ATP synthesis via the TCA cycle, thereby stimulating insulin secretion.

**Characterizations of GDH266C expressed in COS-7 cells and in isolated rat pancreatic islets.** To overexpress GDH266C in isolated rat pancreatic islets, we constructed a recombinant adenovirus, Ad-hGDH266C. As we previously demonstrated using the enzyme expressed in COS-7 cells (22), basal activity (activity in the absence of allosteric effectors) of GDH266C was elevated, and inhibition by GTP and activation by ADP were blunted compared with those of the wild-type enzyme. Here, we further characterized activation by leucine by using COS-7 cell extracts in which wild-type GDH or GDH266C was overexpressed by adenovirus-mediated gene transduction. Activation of GDH266C by leucine was only twofold (from  $2,850 \pm 120$  to  $5,520 \pm 190$  nmol NADH·mg protein<sup>-1</sup>·min<sup>-1</sup> at 3 mmol/l leucine), whereas that of wild-type GDH was more than 35-fold (from  $130 \pm 20$  to  $4,670 \pm 70$  nmol NADH·mg protein<sup>-1</sup>·min<sup>-1</sup> at 3 mmol/l leucine). Maximal activity of GDH266C in the presence of leucine was nearly the same as that of the wild-type enzyme in the crude cell extracts, although analysis of the purified enzyme was necessary for the strict quantitative comparison.

Next, we overexpressed GDH266C in isolated islets (Islets-GDH266C) using the adenovirus-mediated gene transfer system to investigate the role of GDH in native  $\beta$ -cells. Islets overexpressing eGFP (Islets-eGFP) were used as a control. Transfer of exogenous genes with adenovirus vector to islets was very efficient, and most of the islet cells expressed eGFP when they were infected with Ad-eGFP, as confirmed by observation under fluorescence microscopy (Ref. 24 and data not shown). The basal GDH activities in the crude extracts of Islets-eGFP and Islets-GDH266C were  $20 \pm 3$  and  $2,890 \pm 670$  nmol NADH·mg protein<sup>-1</sup>·min<sup>-1</sup>, respectively, when activity was measured without allosteric effectors in the reaction mixture (Table 1). As expected, ADP activated GDH activity 20-fold in the crude extract of Islets-eGFP ( $510 \pm 50$  nmol NADH·mg protein<sup>-1</sup>·min<sup>-1</sup> at 200  $\mu$ mol/l ADP), whereas activation in the extract of Islets-GDH266C was less than twofold ( $4,570 \pm 650$  nmol NADH·mg protein<sup>-1</sup>·min<sup>-1</sup> at 200  $\mu$ mol/l ADP). GTP did not inhibit GDH activity in Islets-GDH266C ( $2,840 \pm 600$  nmol NADH·mg protein<sup>-1</sup>·min<sup>-1</sup> at 25  $\mu$ mol/l GTP). Therefore, in Islets-GDH266C, GDH activity was constitutively elevated.

**Profiles of insulin secretion from Islets-GDH266C.** It is known that in normal pancreatic  $\beta$ -cells glutamine stimulates

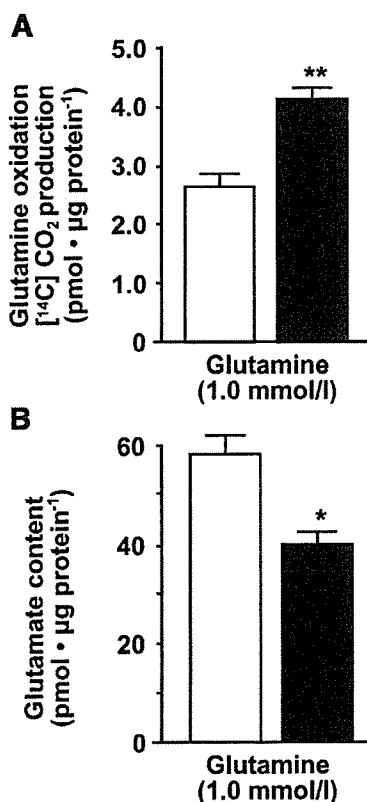


Fig. 1. Glutamine oxidation and glutamate content in MIN6 cells incubated in the presence of glutamine. **A:** glutamine oxidation. MIN6 cells overexpressing constitutively activated mutant glutamate dehydrogenase (GDH; MIN6-GDH266C; filled bar) and MIN6 cells overexpressing lacZ (MIN6-lacZ; open bar) were preincubated in HEPES-balanced Krebs-Ringer bicarbonate buffer (HB-KRBB) with 5 mmol/l glucose for 30 min at 37°C, followed by incubation in HB-KRBB with 1 mmol/l L-[U-<sup>14</sup>C]glutamine for 30 min at 37°C. [<sup>14</sup>C]CO<sub>2</sub> produced by the MIN6 cells was trapped in KOH solution and radioactivity determined by liquid scintillation counting. Data are means  $\pm$  SE of 3 experiments. \*\* $P < 0.02$  for comparison between MIN6-GDH266C and MIN6-lacZ (unpaired Student's *t*-test). **B:** glutamate contents. MIN6-GDH266C (filled bar) and MIN6-lacZ (open bar) cells were preincubated at 37°C in HB-KRBB with 5 mmol/l glucose for 30 min, followed by incubation at 37°C in the presence of 1 mmol/l glutamine for 1 h. Immediately after incubation, cells were quickly homogenized in ice-cold perchloric acid solution. The solution was neutralized and the supernatant saved at  $-80^{\circ}\text{C}$  for the glutamate assay. Glutamate content was determined by HPLC. Data are means  $\pm$  SE of 5 experiments. \* $P < 0.01$  for comparison between MIN6-GDH266C and MIN6-lacZ (unpaired Student's *t*-test).

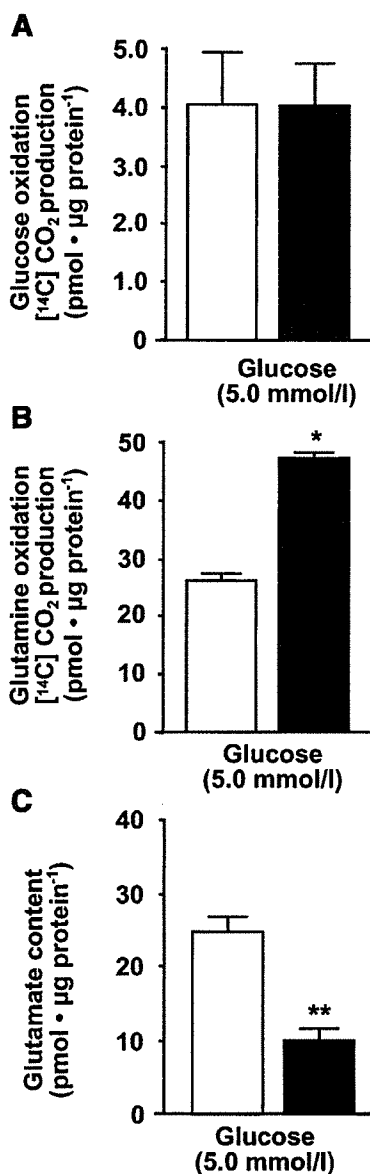


Fig. 2. Glutamine oxidation and glutamate content in MIN6 cells incubated in the presence of 5 mmol/l glucose. *A*: glucose oxidation. MIN6-GDH266C (filled bar) and MIN6-lacZ (open bar) cells were preincubated in HB-KRBB with 5 mmol/l glucose for 30 min at 37°C, followed by incubation in HB-KRBB with 5 mmol/l D-[6-<sup>14</sup>C]glucose for 1 h at 37°C. [<sup>14</sup>C]CO<sub>2</sub> produced by the MIN6 cells was trapped in KOH solution and radioactivity determined by liquid scintillation counting. Data are means ± SE of 6 experiments. *B*: glutamine oxidation. MIN6-GDH266C (filled bar) and MIN6-lacZ (open bar) cells were preincubated at 37°C in HB-KRBB with 5 mmol/l glucose for 30 min, followed by incubation at 37°C for 30 min in the presence of 5 mmol/l glucose and a tracer of radioactive L-[U-<sup>14</sup>C]glutamine. Radioactive [<sup>14</sup>C]CO<sub>2</sub> produced by the MIN6 cells was trapped in KOH solution and radioactivity determined by liquid scintillation counting. Data are means ± SE of 3 experiments. \**P* < 0.001 for comparison between MIN6-GDH266C and MIN6-lacZ (unpaired Student's *t*-test). *C*: glutamate contents. MIN6-GDH266C (filled bar) and MIN6-lacZ (open bar) cells were preincubated at 37°C in HB-KRBB with 5 mmol/l glucose for 30 min, followed by incubation at 37°C in the presence of 5 mmol/l glucose for 1 h. After incubation, glutamate contents were measured as described in Fig. 1. Data are means ± SE of 5 experiments. \*\**P* < 0.002 for comparison between MIN6-GDH266C and MIN6-lacZ (unpaired Student's *t*-test).

Table 1. GDH activity in Islets-GDH266C and Islets-eGFP

ADP, µmol/l	GTP, µmol/l	GDH Activity, nmol NADH·mg protein <sup>-1</sup> ·min <sup>-1</sup>	
		Islets-eGFP	Islets-266C
0	0	20 ± 3	2,890 ± 670
200	0	510 ± 50	4,570 ± 650
0	25	*	2,840 ± 600

Values are means ± SE; *n* = 3. GDH, glutamate dehydrogenase; Islets-GDH266C, islets overexpressing a constitutively activated mutant GDH; Islets-eGFP, islets overexpressing enhanced green fluorescent protein (control). \*Below assay sensitivity.

insulin secretion only in the presence of leucine, an allosteric activator of GDH. As shown in Fig. 3*A*, glutamine alone did not stimulate insulin secretion from Islets-eGFP, as was observed with intact islets. On the other hand, it stimulated insulin secretion from Islets-GDH266C in a dose-dependent manner.

Glucose-stimulated insulin secretion was also studied. Insulin secretion from Islets-GDH266C was significantly exaggerated at low glucose concentrations compared with control Islets-eGFP [0.16 ± 0.03 (Islets-eGFP) vs. 0.34 ± 0.09 ng insulin/µg protein (Islets-GDH266C) at 2 mmol/l glucose (*P* < 0.05, *n* = 16); 0.29 ± 0.06 (Islets-eGFP) vs. 0.48 ± 0.07 ng insulin/µg protein (Islets-GDH266C) at 5 mmol/l glucose (*P* < 0.001, *n* = 15); 0.55 ± 0.08 (Islets-eGFP) vs. 0.78 ± 0.15 ng insulin/µg protein (Islets-GDH266C) at 8 mmol/l glucose (*P* < 0.05, *n* = 14); paired *t*-test] but not at higher glucose concentrations (Fig. 3*B*).

DISCUSSION

A mutant GDH, GHD266C, which was identified in a Japanese patient with HI/HA syndrome, is a constitutively activated enzyme: basal activity is elevated, and activation by ADP and inhibition by GTP are blunted compared with the wild-type enzyme (22). In addition, we have herein demonstrated activation by leucine also to be blunted. It has been suggested that ADP binds to and activates GDH by opening the catalytic cleft of the enzyme (16). Leucine is thought to bind at the active site (26). It is possible that in GDH266C the catalytic cleft is almost fully open in the basal state, such that binding of ADP or leucine only minimally activates this mutant enzyme. We used the GDH266C, rather than wild-type GDH, as a tool to examine the effects of elevated cellular GDH activity in the regulation of insulin secretion, because with this mutant, GDH activity is thought to be elevated regardless of phosphate potential (GTP and ATP-to-ADP and P<sub>i</sub> ratio) (2, 5) in the cells.

We previously demonstrated glutamine to stimulate insulin secretion from MIN6 cells overexpressing GDH266C (MIN6-GDH266C) in the absence of leucine. In addition, and very interestingly, insulin secretion from MIN6-GDH266C cells was exaggerated at low glucose concentrations (2–5 mmol/l) in the absence of glutamine in the incubation buffer (22). To investigate the mechanism by which elevated cellular GDH activity leads to the stimulation of insulin secretion, we studied changes in glutamate metabolism in cells in which GDH activity was constitutively elevated.

In association with the stimulation of insulin secretion by glutamine, cellular glutamine oxidation was elevated (Fig. 1*A*),



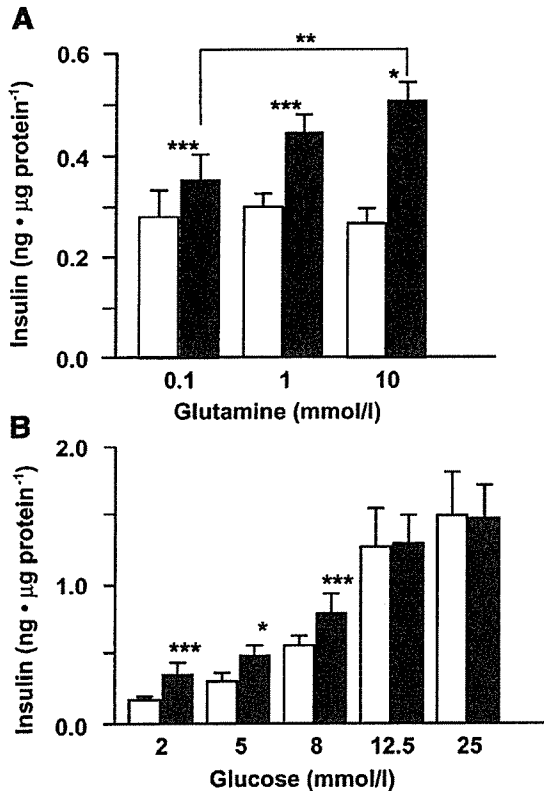


Fig. 3. Glutamine- and glucose-stimulated insulin secretion. *A*: glutamine-stimulated insulin secretion. After a 30-min preincubation in the buffer with 5 mmol/l glucose and without glutamine, pancreatic islets overexpressing GDH266C (Islets-GDH266C; filled bar) and islets overexpressing enhanced green fluorescent protein (Islets-eGFP; open bar) were incubated in the presence of various concentrations of glutamine (without glucose) for 30 min, and insulin released into the incubation buffer was measured. Each assay was performed using 10–30 islets, and values are means  $\pm$  SE of 3–7 experiments. \* $P < 0.01$  and \*\*\* $P < 0.05$  for comparison between Islets-GDH266C and Islets-eGFP. \*\* $P < 0.02$  for comparison between 0.1 and 10 mmol/l glutamine (Islets-GDH266C) (paired Student's *t*-tests). *B*: glucose-stimulated insulin secretion. After preincubation, Islets-GDH266C (filled bar) and Islets-eGFP (open bar) were incubated in the presence of various concentrations of glucose for 30 min, and insulin released into the incubation buffer was measured. Each assay was performed using 10–30 islets, and values are means  $\pm$  SE of 6–16 experiments. \* $P < 0.01$  and \*\*\* $P < 0.05$  for comparison between Islets-GDH266C and Islets-eGFP (paired Student's *t*-tests).

and intracellular glutamate content was lower (Fig. 1*B*) in MIN6-266C cells. This observation is consistent with the hypothesis that elevated GDH activity enhances the oxidative deamination of glutamate to  $\alpha$ -ketoglutarate to supply TCA cycle substrates (18, 19). It is noteworthy that, at the basal glucose concentration (5 mmol/l) without glutamine in the medium, exaggerated insulin secretion was also associated with enhanced glutamine oxidation, and a decrease in the intracellular glutamate content reflected utilization of the substrate. At this glucose concentration, glutamine (or glutamate) from the intracellular pool would likely be utilized as a substrate of GDH to fuel the TCA cycle and thereby stimulate insulin secretion. At a higher glucose concentration (25 mmol/l), glutamine oxidation also increased, and the cellular glutamate content was lower in MIN6-GDH266C than in MIN6-lacZ cells, although insulin secretion did not differ. Under

these conditions, the effect of increased glutamate oxidation on insulin secretion was probably undetectable because glucose stimulation was more potent.

Although the MIN6 cell line is one of the best models of native  $\beta$ -cells (13), it is derived from an insulinoma, and insulin-secretory profiles are known to change over several passages (12). Therefore, this cell line may not adequately reflect native  $\beta$ -cells in some respects. Therefore, we wished to confirm the effect of unregulated elevation of GDH activity on insulin secretion in a more physiological model: isolated rat pancreatic islets. Islets-GDH266C secreted insulin in response to glutamine in a dose-dependent manner (Fig. 3*A*). More importantly, in Islets-GDH266C, insulin secretion was also significantly enhanced at low glucose concentrations (2–8 mmol/l) compared with control Islets-eGFP (Fig. 3*B*), just as we observed in MIN6-GDH266C cells (22). Recently, Kelly et al. (5) reported an H454Y-GDH transgenic mouse. In this animal model, an HI/HA syndrome patient-derived mutant, H454Y-GDH, the activity of which was not inhibited by GTP, was specifically expressed in  $\beta$ -cells. Random blood glucose concentrations were lower than in control mice, and amino acid- and leucine-stimulated insulin secretions from perfused islets were markedly enhanced in these mice. Although glucose-stimulated insulin secretion was reported to be similar to that of control mouse islets, detailed data, including basal insulin secretion at low glucose concentrations, have not been presented. Because basal GDH activity was more than 100 times higher than that in control islets in our model (Table 1), the enhancement of basal insulin secretion might have been more prominent in our model than in the transgenic mouse model.

Physiologically, GDH is an important regulator of glutaminolysis (glutamine oxidation), which may contribute to the interprandial basal insulin secretion (2, 5). Glutaminolysis is regulated by allosteric regulation of GDH with amino acids such as leucine, isoleucine, and methionine. In addition, it is also precisely regulated by glucose metabolism through changes in concentrations of other important allosteric regulators of GDH, GTP, ATP, and ADP. According to this hypothesis, at glucose concentrations near or below its threshold to stimulate insulin secretion (5 mmol/l), GDH is activated by a decrease in the GTP/ADP ratio and drives basal insulin secretion, at least in part (2, 5). Insulin-secretory profiles of MIN6-GDH266C cells and Islets-GDH266C are in agreement with this hypothesis. Constitutively activated GDH rendered the cells responsive to glutamine in insulin secretion in the absence of leucine and enhanced insulin secretion at low glucose concentrations. Furthermore, they would be reflected in the fasting and protein meal-induced hyperinsulinemic hypoglycemia in patients with HI/HA syndrome, although in patients'  $\beta$ -cells elevation of GDH activity at low glucose concentrations would be modest compared with that in MIN6-GDH266C cells and in Islets-GDH266C. On the other hand, in our previous and present studies, glucose-stimulated insulin secretion was not enhanced in either MIN6-GDH266C cells (22) or Islets-GDH266C (Fig. 3*B*). On the basis of the insulin secretion profiles and glutamate metabolism, our data do not support the hypothesis that glutamate, derived from the reverse GDH reaction (flux from  $\alpha$ -ketoglutarate to glutamate), is a second messenger of glucose-stimulated insulin secretion (1, 2, 5, 8, 9), although we neither measured the flux directly nor tested

the messenger action of glutamate in glucose-stimulated insulin secretion, and therefore the messenger role of glutamate is not completely excluded.

This is the first study, to our knowledge, in which insulin secretion and glutamate metabolism were analyzed simultaneously under conditions of direct and constitutive cellular GDH activity elevation. Our results illustrate the importance of GDH in amino acid-stimulated insulin secretion and possible contribution to the regulation of basal insulin secretion. Furthermore, we have provided additional evidence that, at least under our experimental conditions, the metabolic flux through GDH is in the direction of  $\alpha$ -ketoglutarate production in pancreatic  $\beta$ -cells. No evidence was obtained to suggest that glutamate produced by the reverse GDH reaction enhanced insulin secretion.

#### ACKNOWLEDGMENTS

We thank Prof. Jun-ichi Miyazaki, Osaka University, Japan, for providing us with MIN6 cells. We are grateful to Atsuko Tanimura, Yukari Kora-Miura, and Mayumi Kaneko for expert technical assistance.

#### GRANTS

This study was supported in part by Grants-in-Aid for Creative Scientific Research (10NP0201 to Y. Oka) and for Scientific Research (14370338 to Y. Tanizawa) from the Ministry of Education, Culture, Sports, Science and Technology of Japan.

#### REFERENCES

- Bertrand G, Ishiyama N, Nenquin M, Ravier MA, and Henquin JC. The elevation of glutamate content and the amplification of insulin secretion in glucose-stimulated pancreatic islets are not causally related. *J Biol Chem* 277: 32883–32891, 2002.
- Gao ZY, Li G, Najafi H, Wolf BA, and Matschinsky FM. Glucose regulation of glutaminolysis and its role in insulin secretion. *Diabetes* 48: 1535–1542, 1999.
- Godel H, Graser T, Foldi P, Pfaender P, and Furst P. Measurement of free amino acids in human biological fluids by high-performance liquid chromatography. *J Chromatogr* 297: 49–61, 1984.
- Hoy M, Maechler P, Efanov AM, Wollheim CB, Berggren PO, and Gromada J. Increase in cellular glutamate levels stimulates exocytosis in pancreatic beta-cells. *FEBS Lett* 531: 199–203, 2002.
- Kelly A, Li C, Gao Z, Stanley CA, and Matschinsky FM. Glutaminolysis and insulin secretion: from bedside to bench and back. *Diabetes* 51, Suppl 3: S421–S426, 2002.
- Lacy PE and Kostianovsky M. Method for the isolation of intact islets of Langerhans from the rat pancreas. *Diabetes* 16: 35–39, 1967.
- Liu YJ, Cheng H, Drought H, MacDonald MJ, Sharp GW, and Straub SG. Activation of the  $K_{ATP}$  channel-independent signaling pathway by the nonhydrolyzable analog of leucine, BCH. *Am J Physiol Endocrinol Metab* 285: E380–E389, 2003.
- MacDonald MJ and Fahien LA. Glutamate is not a messenger in insulin secretion. *J Biol Chem* 275: 34025–34027, 2000.
- MacMullen C, Fang J, Hsu BY, Kelly A, de Lonlay-Debeney P, Saudubray JM, Ganguly A, Smith TJ, and Stanley CA. Hyperinsulinism/hyperammonemia syndrome in children with regulatory mutations in the inhibitory guanosine triphosphate-binding domain of glutamate dehydrogenase. *J Clin Endocrinol Metab* 86: 1782–1787, 2001.
- Maechler P, Gjinovci A, and Wollheim CB. Implication of glutamate in the kinetics of insulin secretion in rat and mouse perfused pancreas. *Diabetes* 51, Suppl 1: S99–S102, 2002.
- Maechler P and Wollheim CB. Mitochondrial glutamate acts as a messenger in glucose-induced insulin exocytosis. *Nature* 402: 685–689, 1999.
- Minami K, Yano H, Miki T, Nagashima K, Wang CZ, Tanaka H, Miyazaki JI, and Seino S. Insulin secretion and differential gene expression in glucose-responsive and -unresponsive MIN6 sublines. *Am J Physiol Endocrinol Metab* 279: E773–E781, 2000.
- Miyazaki J, Araki K, Yamato E, Ikegami H, Asano T, Shibasaki Y, Oka Y, and Yamamura K. Establishment of a pancreatic beta cell line that retains glucose-inducible insulin secretion: special reference to expression of glucose transporter isoforms. *Endocrinology* 127: 126–132, 1990.
- Mizuguchi H and Kay MA. Efficient construction of a recombinant adenovirus vector by an improved in vitro ligation method. *Hum Gene Ther* 9: 2577–2583, 1998.
- Mizuguchi H and Kay MA. A simple method for constructing E1- and E1/E4-deleted recombinant adenoviral vectors. *Hum Gene Ther* 10: 2013–2017, 1999.
- Peterson PE and Smith TJ. The structure of bovine glutamate dehydrogenase provides insights into the mechanism of allosteric regulation. *Structure Fold Des* 7: 769–782, 1999.
- Rubi B, Ishihara H, Hegardt FG, Wollheim CB, and Maechler P. GAD65-mediated glutamate decarboxylation reduces glucose-stimulated insulin secretion in pancreatic beta cells. *J Biol Chem* 276: 36391–36396, 2001.
- Sener A and Malaisse WJ. L-Leucine and a nonmetabolized analogue activate pancreatic islet glutamate dehydrogenase. *Nature* 288: 187–189, 1980.
- Sener A, Malaisse-Lagae F, and Malaisse WJ. Stimulation of pancreatic islet metabolism and insulin release by a nonmetabolizable amino acid. *Proc Natl Acad Sci USA* 78: 5460–5464, 1981.
- Stanley CA, Fang J, Kutyna K, Hsu BY, Ming JE, Glaser B, and Poncez M. Molecular basis and characterization of the hyperinsulinism/hyperammonemia syndrome: predominance of mutations in exons 11 and 12 of the glutamate dehydrogenase gene. *Diabetes* 49: 667–673, 2000.
- Stanley CA, Lieu YK, Hsu BY, Burlina AB, Greenberg CR, Hopwood NJ, Perlman K, Rich BH, Zammarchi E, and Poncez M. Hyperinsulinism and hyperammonemia in infants with regulatory mutations of the glutamate dehydrogenase gene. *N Engl J Med* 338: 1352–1357, 1998.
- Tanizawa Y, Nakai K, Sasaki T, Anno T, Ohta Y, Inoue H, Matsuo K, Koga M, Furukawa S, and Oka Y. Unregulated elevation of glutamate dehydrogenase activity induces glutamine-stimulated insulin secretion: identification and characterization of a GLUD1 gene mutation and insulin secretion studies with MIN6 cells overexpressing the mutant glutamate dehydrogenase. *Diabetes* 51: 712–717, 2002.
- Tanizawa Y, Ohta Y, Nomiya J, Matsuda K, Tanabe K, Inoue H, Matsutani A, Okuya S, and Oka Y. Overexpression of dominant negative mutant hepatocyte nuclear factor (HNF)-1 $\alpha$  inhibits arginine-induced insulin secretion in MIN6 cells. *Diabetologia* 42: 887–891, 1999.
- Ueda K, Tanizawa Y, Ishihara H, Kizuki N, Ohta Y, Matsutani A, and Oka Y. Overexpression of mitochondrial FAD-linked glycerol-3-phosphate dehydrogenase does not correct glucose-stimulated insulin secretion from diabetic GK rat pancreatic islets. *Diabetologia* 41: 649–653, 1998.
- Weinzimer SA, Stanley CA, Berry GT, Yudkoff M, Tuchman M, and Thornton PS. A syndrome of congenital hyperinsulinism and hyperammonemia. *J Pediatr* 130: 661–664, 1997.
- Wrzeszczynski KO and Colman RF. Activation of bovine liver glutamate dehydrogenase by covalent reaction of adenosine 5'-O-[S-(4-bromo-2,3-dioxobutyl)thiophosphate] with arginine-459 at an ADP regulatory site. *Biochemistry* 33: 11544–11553, 1994.
- Yamada H, Yamamoto A, Yodozawa S, Kozaki S, Takahashi M, Morita M, Michibata H, Furuichi T, Mikoshiba K, and Moriyama Y. Microvesicle-mediated exocytosis of glutamate is a novel paracrine-like chemical transduction mechanism and inhibits melatonin secretion in rat pinealocytes. *J Pineal Res* 21: 175–191, 1996.
- Yamada S, Komatsu M, Sato Y, Yamauchi K, Aizawa T, and Hashizume K. Glutamate is not a major conveyer of ATP-sensitive  $K^+$  channel-independent glucose action in pancreatic islet beta cell. *Endocr J* 48: 391–395, 2001.
- Zammarchi E, Filippi L, Novembre E, and Donati MA. Biochemical evaluation of a patient with a familial form of leucine-sensitive hypoglycemia and concomitant hyperammonemia. *Metabolism* 45: 957–960, 1996.

## Carboxy Terminus of Glucose Transporter 3 Contains an Apical Membrane Targeting Domain

KOUICHI INUKAI, ANNETTE M. SHEWAN, WENDY S. PASCOE, SHIGEHIRO KATAYAMA, DAVID E. JAMES, AND YOSHITOMO OKA

*Fourth Department of Internal Medicine (K.I., S.K.), Saitama Medical School, Saitama 350-0495, Japan; and Division of Molecular Metabolism and Diabetes (Y.O.), Department of Internal Medicine Tohoku University Graduate School of Medicine, Miyagi 980-8574, Japan; Institute for Molecular Bioscience (A.M.S., W.S.P., D.E.J.), University of Queensland, Brisbane 4072, Australia; and Garvan Institute of Medical Research (D.E.J.), St. Vincents Hospital, Sydney 2010, Australia*

We previously demonstrated that distinct facilitative glucose transporter isoforms display differential sorting in polarized epithelial cells. In Madin-Darby canine kidney (MDCK) cells, glucose transporter 1 and 2 (GLUT1 and GLUT2) are localized to the basolateral cell surface whereas GLUTs 3 and 5 are targeted to the apical membrane. To explore the molecular mechanisms underlying this asymmetric distribution, we analyzed the targeting of chimeric glucose transporter proteins in MDCK cells. Replacement of the carboxy-terminal cytosolic tail of GLUT1, GLUT2, or GLUT4 with that from GLUT3 resulted in apical targeting. Conversely, a GLUT3 chimera containing the cytosolic carboxy terminus of GLUT2 was sorted to the basolateral membrane. These findings are not attributable to the presence

of a basolateral signal in the tails of GLUTs 1, 2, and 4 because the basolateral targeting of GLUT1 was retained in a GLUT1 chimera containing the carboxy terminus of GLUT5. In addition, we were unable to demonstrate the presence of an autonomous basolateral sorting signal in the GLUT1 tail using the low-density lipoprotein receptor as a reporter. By examining the targeting of a series of more defined GLUT1/3 chimeras, we found evidence of an apical targeting signal involving residues 473–484 (DRSGKDGVMEMN) in the carboxy tail. We conclude that the targeting of GLUT3 to the apical cell surface in MDCK cells is regulated by a unique cytosolic sorting motif. (*Molecular Endocrinology* 18: 339–349, 2004)

THE DELIVERY SYSTEM for the targeting of membrane proteins to different cell surfaces in polarized cells has been a subject of considerable interest. Many studies have concentrated on identifying the determinants of basolateral and apical sorting signals at the molecular level (1, 2). A number of basolateral sorting signals described to date have been found to reside in the cytoplasmic domain of membrane proteins (3, 4). Most belong to two classes characterized by either a critical tyrosine-containing motif (YXXØ) (5) or a dileucine or leucine residue adjacent to another bulky hydrophobic amino acid (a.a.) (6, 7). These signals have been demonstrated to associate with adaptor protein 1 (8) and adaptor protein 2 (9, 10), which regulate clathrin assembly at the trans-Golgi network and the plasma membrane, respectively. These signals appear to mediate both efficient delivery to the basolateral membrane and endocytic recycling. Conversely, most of the apical signals that have been characterized to date are found in luminal or trans-membrane domains. Although relatively little is known

about apical sorting signals, both N-linked (11, 12) and O-linked glycosylation (13, 14) have been shown to play an important role.

Facilitative hexose transporters constitute a family of integral membrane proteins that mediate the transport of sugars across cellular membranes (15). These isoforms share a high level of a.a. sequence homology, and their predicted three-dimensional structure is conserved. Considerable evidence suggests that they contain 12 transmembrane domains with both the N and C termini located on the cytosolic side (15). Despite these similarities, major differences in intracellular trafficking have been noted between individual GLUTs. These differences are best demonstrated in polarized cell types in which different transporters have been localized to discrete surfaces. Glucose transporter 1 and 2 (GLUT1 and GLUT2) are principally found on the basolateral surface in epithelial cells whereas GLUT3 and GLUT5 are mainly targeted to the apical domain (16–19). Similar results are obtained when these transporter isoforms are transfected into Madin-Darby canine kidney (MDCK) cells indicating that this is a universal feature of these proteins that can be recapitulated in a heterologous system (20). These results also demonstrate that MDCK cells provide a useful model for studying the vectorial membrane trafficking of facilitative hexose transporters.

Abbreviations: a.a., Amino acid(s); GLUT, glucose transporter; LDL-R, low-density lipoprotein receptor; MDCK, Madin-Darby canine kidney.

***Molecular Endocrinology*** is published monthly by The Endocrine Society (<http://www.endo-society.org>), the foremost professional society serving the endocrine community.

The asymmetric distribution of GLUTs in polarized cell types has physiological relevance. For example, with respect to the intestinal absorption of fructose, the apically targeted GLUT5 exhibits a high affinity for fructose [low Michaelis-Menten constant ( $K_m$ )] (21), whereas the basolaterally targeted GLUT2 exhibits a high  $V_{max}$  for fructose (22). Hence, these two facilitative transporters cooperate to achieve efficient absorption of fructose across the gut epithelium.

The molecular mechanisms by which GLUTs are differentially targeted in polarized cells remain to be clarified. Therefore, we attempted to characterize the structural determinants of GLUTs required for this differential targeting. We have expressed a panel of chimeric transporters utilizing various portions of GLUTs 1–5 in MDCK cells and assessed their differential distribution. Our data show that the carboxy-terminal tail of human (h)GLUT3 contains a dominant apical sorting signal that is capable of rerouting both GLUT1 and GLUT2 from the basolateral to the apical cell surface in MDCK cells.

## RESULTS

### Expression and Analysis of GLUT1/3 Chimeras in MDCK Cells

To clarify the molecular basis for the differential targeting of GLUTs in polarized epithelial cells, we undertook a chimeric strategy whereby different portions of a basolateral transporter and an apical transporter were spliced together and expressed in MDCK cells. Initially, we focused on hGLUT1 and hGLUT3, which are targeted to the basolateral and apical cell surfaces, respectively, in MDCK cells (20). MDCK cells express GLUT1 endogenously but not GLUT3 (20). Initially, we studied the targeting of recombinant hGLUT1 when overexpressed in MDCK cells. Stable cell lines were selected and screened for hGLUT1 expression using a monoclonal antibody that is specific for hGLUT1 (23). This antibody recognizes an epitope in the central loop of hGLUT1 and provides a useful tool for comparing relative expression levels between individual constructs and clones. To verify that this expression system did not result in marked overexpression, we analyzed the glucose transport activities of these clones. In wild-type cells, we observed glucose transport rates of  $0.77 \pm 0.16$  nmol/mg·min and  $0.04 \pm 0.06$  nmol/mg·min across the basolateral and apical membranes, respectively ( $n = 5$ , mean  $\pm$  sd). The glucose transport rates across the basolateral membranes in GLUT1-expressing cell lines were increased at most by 1.5-fold as compared with that observed in wild-type cells. Moreover, we did not observe a significant change in apical transport in clones expressing GLUT1 at this expression level. On the other hand, in clones expressing GLUT3 over a broad range of expression

levels, we observed a highly significant increase in transport across the apical membrane ( $0.56 \pm 0.10$  nmol/mg·min). Thus, these data provide a good indication that we have performed our studies using non-saturating expression levels of recombinant transporters. As shown in Fig. 1C (*left upper panel*), at this level of expression the targeting of hGLUT1 was restricted to the basolateral surface as was the case for the endogenous protein. Also shown in Fig. 1C (*right upper panel*) is the distribution of hGLUT3 expressed in MDCK cells. Consistent with our previous findings (20), this protein was highly enriched at the apical cell surface. Whereas these transporters localize to either basolateral or apical membranes, intracellular labeling is also evident. Our focus in this study was the contribution of the cytosolic carboxy terminus to domain-specific cell surface localization and as such we did not characterize the intracellular vesicular compartments through which these chimeras traffic.

The above data provided the basis for our initial studies using hGLUT1/3 chimeras expressed in MDCK cells. We first designed two GLUT1/3 chimeras comprised of different portions of both proteins: hGLUT1/3CT290 contains the N-terminal half of hGLUT1 and the C-terminal half of GLUT3; and hGLUT1/3CT36 is comprised of hGLUT1 in which the carboxy-terminal tail (32 a.a.) has been replaced with that of hGLUT3 (36 a.a.). A scheme of these and other constructs is shown in Fig. 1A. As was the case for all of the constructs described in this study, we selected at least 12 different stable cell lines expressing the recombinant protein of interest and performed detailed analyses on at least three to four different clones for each construct covering a range of expression levels. The targeting of endogenous GLUT1, as well as inulin exclusion, was analyzed in each clone to verify polarity at the time of study (data not shown). Figure 1B shows a Western blot of cell lysates from cells expressing either full-length GLUT3 or the relevant chimeras using an antibody raised against the C-terminal domain of hGLUT3. This antibody did not detect a specific signal in non-transfected MDCK cells, but clearly detected the exogenous hGLUT3 epitope. The chimeras yielded proteins of the appropriate molecular size, *i.e.* similar to that observed for full-length GLUT3. Figure 1C shows the immunolocalization of the hGLUT1/3CT290 (*left lower panel*) and hGLUT1/3CT36 (*right lower panel*) chimeras in MDCK cells as compared with both GLUT1 and GLUT3. Both chimeras were concentrated on the apical domain, similar to the targeting observed for the full-length GLUT3 protein. We also observed labeling of intracellular structures (Fig. 1). This is consistent with our previous studies in which even GLUT1, which is highly concentrated on the basolateral surface (Fig. 1), was also found in intracellular vesicles in MDCK cells (20). These results suggest that the carboxy tails of these transporter proteins determine basolateral vs. apical delivery.

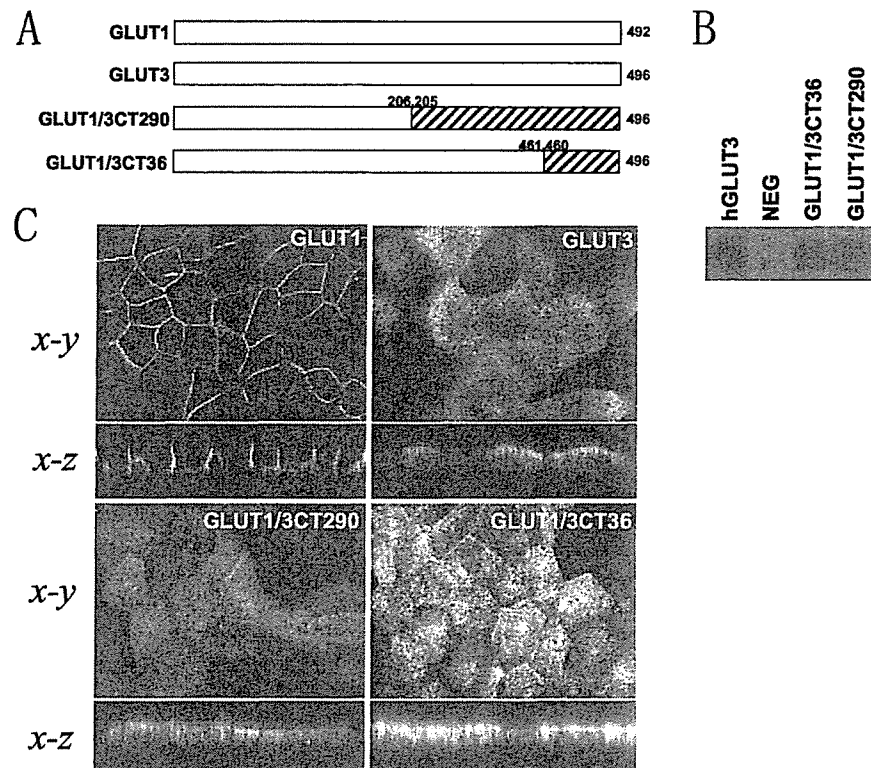


**Fig. 1.** Immunofluorescence Localizations of GLUT1 and GLUT3 and Their Chimeric GLUTs

A, A diagrammatic representation of the constructs used in these studies is shown. B, Total membrane samples (15  $\mu$ g) prepared from MDCK cells expressing the indicated proteins were subjected to SDS-PAGE and immunoblotting with an antibody raised against the C-terminal domain of GLUT3. NEG refers to a sample prepared in parallel from parental MDCK cells. Immunoblot data identical to those presented for parental membranes were obtained from nonexpressing but G418-resistant MDCK clones. C, MDCK cells expressing the indicated proteins were plated on glass coverslips, and immunofluorescence was performed as previously described (20). Exogenous transporters were detected using an antibody raised against a short peptide derived from the intracellular loop of hGLUT1 (GLUT1) and an antibody raised against the C-terminal domain of GLUT3 (GLUT3, GLUT1/3CT290, and GLUT1/3CT36). Confocal images were generated using a Zeiss Axiophot fluorescent microscope and a Bio-Rad MRC600 laser scanning head.

#### Expression of a Low-Density Lipoprotein Receptor (LDL-R)/GLUT1 Chimera in MDCK Cells

It was shown previously that the cytoplasmic tail of the LDL-R possesses two tyrosine-dependent basolateral targeting signals (24, 25). Deletion of these residues resulted in rerouting of the LDL-R to the apical cell surface (24). To determine whether the GLUT1 carboxy tail possesses a basolateral sorting signal, we studied the trafficking of an LDL-R chimera containing the carboxy tail of GLUT1 (LDL-R/G1CT24), in MDCK cells. Several clones expressing the full-length LDL-R and the chimeras were obtained and grown on transwell filters. Trafficking of these proteins was analyzed using a cell surface biotinylation assay (Fig. 2). In agreement with previous studies (24), the wild-type LDL-R was almost entirely targeted to the basolateral membrane, whereas more than 85% of mutated LDL-R (CT37Y-A18) was targeted to the apical membrane. When 24 a.a. from the C terminus of GLUT1 were grafted onto CT37Y-A18, a small portion of the apical proteins relocated to the basolateral mem-

brane, but the majority remained at the apical membrane (Fig. 2C). These findings suggest that the C-terminal tail of GLUT1 does not contain an autonomous basolateral sorting signal. This does not exclude the possibility of a basolateral sorting signal elsewhere in the GLUT1 molecule. In fact, this seems likely given that it is a multispanning membrane protein with at least three major cytosolic domains. It is also conceivable that sorting domains in these more complex molecules are comprised of discontinuous elements found in discrete domains that interact *in vivo*.

#### Trafficking of a GLUT1/5 Chimera in MDCK Cells

It was shown previously that GLUT5 is targeted to the apical cell surface in polarized epithelial cells and that apical targeting is regulated via information contained within the central portion of the protein (26). Thus, it is highly unlikely that the C-terminal tail of GLUT5 contains targeting information relevant to trafficking in polarized epithelial cells. Therefore, we reasoned that a GLUT1 chimera containing the C terminus of GLUT5

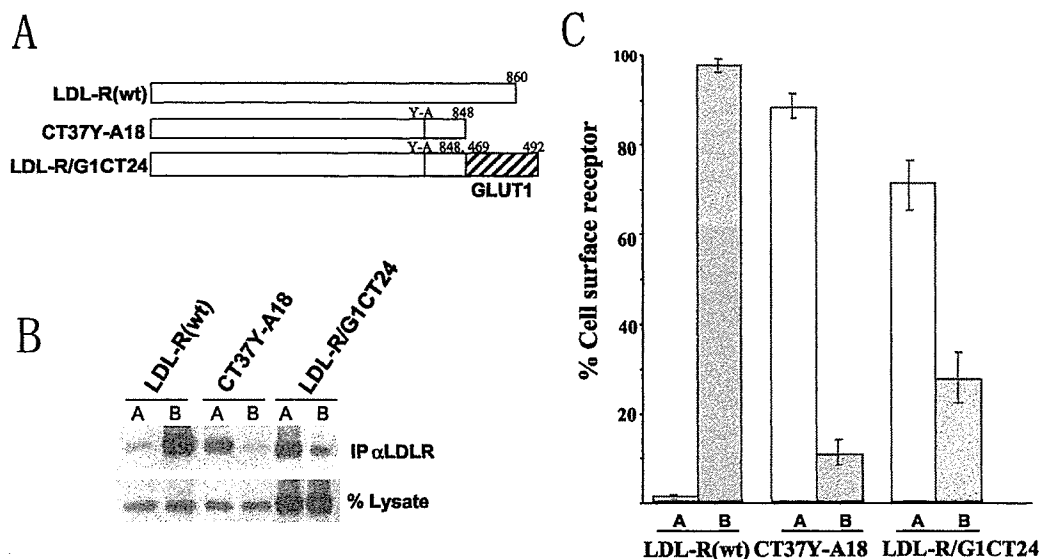


**Fig. 2.** Cell Surface Distributions of Wild and Mutated LDL-Rs Using Biotinylation Assay  
 A, A diagrammatic representation of the constructs used in these studies is shown. B, MDCK cells expressing various chimeric proteins were plated onto transwell filters. Apical (A) or basal (B) cell surfaces were incubated in 0.5 mg/ml EZ-link Sulfo-NHS-biotin (Pierce Chemical Co.) for 15 min on ice. Filters were quenched and transferred into lysis buffer, and the solubilized material was cleared by centrifugation. An aliquot of cleared supernatant served as the total expression sample, and the remainder was incubated with streptavidin-agarose to recover biotinylated proteins. Immunoprecipitated proteins were subjected to SDS-PAGE and subsequent Western blot analysis using a polyclonal LDL-R antibody, LB1, with detection performed using goat antirabbit-horseradish peroxidase antibody and enhanced chemiluminescence. C, Values are given as the percent of total cell surface receptors. Bars represent the mean  $\pm$  sd of three independent experiments.

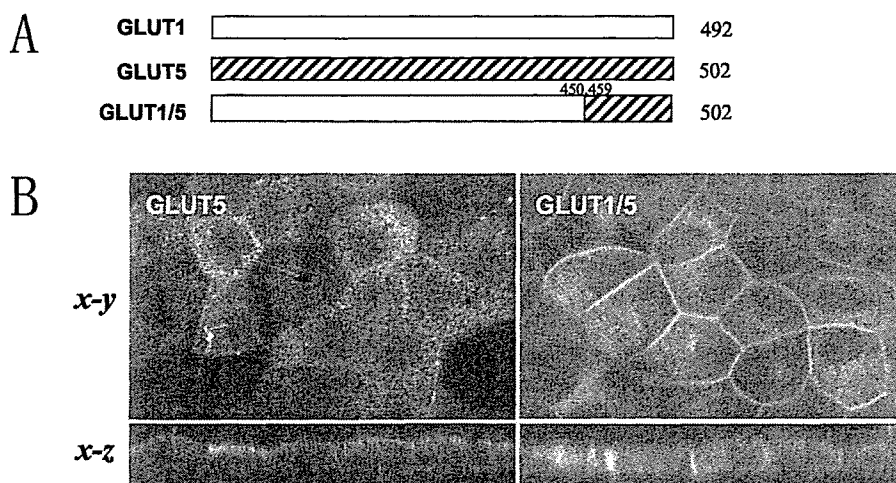


**Fig. 3.** Immunofluorescence Localizations of GLUT5 and GLUT1/5 Chimeric GLUTs  
 A, Scheme of the constructs generated for this analysis. B, MDCK cells expressing the indicated proteins were plated onto flamed, glass coverslips and incubated for 5 d to enable tight junction formation and establishment of polarity. Cells were fixed and the domain-specific localizations of exogenous GLUT5 and the GLUT1/5 chimera were assessed by immunofluorescent microscopy using an antibody raised against the C-terminal domain of GLUT5. The GLUT1/5 chimera consists of residues 1-450 of hGLUT1 joined in frame to residues 459-502 of GLUT5.

should provide a useful tool for the present studies. If this chimera targets to the apical cell surface, this will provide definitive proof that the GLUT1 tail contains a basolateral sorting motif. This chimera was expressed in MDCK cells and localized by immunofluorescence microscopy. As shown in Fig. 3, whereas full-length

GLUT5 was targeted to the apical surface, the GLUT1/5 chimera was found almost exclusively on the basolateral membrane. In combination with the studies described above, these data strongly indicate that the C-terminal tail of GLUT1 does not contain a basolateral targeting motif.

### Expression and Analysis of GLUT2/3 Chimeras in MDCK Cells

To further investigate the apical sorting signal in the C terminus of GLUT3, we undertook an analysis of a panel of chimeras based on hGLUT2 and hGLUT3. Like GLUT1, GLUT2 is targeted to the basolateral cell surface in MDCK cells (20). Initially, we analyzed the targeting of two chimeras, which contained reciprocal portions of GLUT2 and 3. The first, designated GLUT2/3, comprised hGLUT2 up to the end of the last transmembrane domain followed by the cytosolic C-terminal tail of hGLUT3. The second chimera, hGLUT3/2, comprised hGLUT3 up to and including the last transmembrane domain followed by the cytosolic tail of hGLUT2 (Fig. 4A). Both chimeras produced protein products of the correct molecular size when transfected into MDCK cells (data not shown). Confocal immunofluorescence microscopy was used to analyze the targeting of both chimeras in MDCK cells. As shown in Fig. 4B, GLUT2/3 (*left lower panel*) was targeted to the apical membrane and GLUT3/2 (*right lower panel*) to the basolateral membrane. These re-

sults support the conclusion that the cytoplasmic carboxy tail of GLUT3 possesses an autonomous apical targeting motif.

### Expression and Analysis of GLUT4/3 Chimeras in MDCK Cells

We have previously shown that a chimera composed of the full-length GLUT4 protein and the last 12 a.a. of hGLUT3 appended to the C terminus of GLUT4, when expressed in adipocytes, behaves indistinguishably from GLUT4 (27). This chimera, termed GLUT4/3<sub>tag</sub>, was expressed in MDCK cells and found to be targeted to intracellular membranes (Fig. 5C, *left panel*) in a manner similar to that previously described for the wild-type GLUT4 protein (20). The intracellular sequestration of GLUT4 is controlled, in part, by an aromatic a.a.-based signal (FQQI) in the cytosolic N terminus of the protein (28). Phenylalanine at position 5 was mutated to alanine in this GLUT4/3<sub>tag</sub> chimera and expressed in MDCK cells. Localization studies indicated that some GLUT4/3<sub>tag</sub>F5A was targeted to the basolateral cell surface, whereas others stayed in an intra-

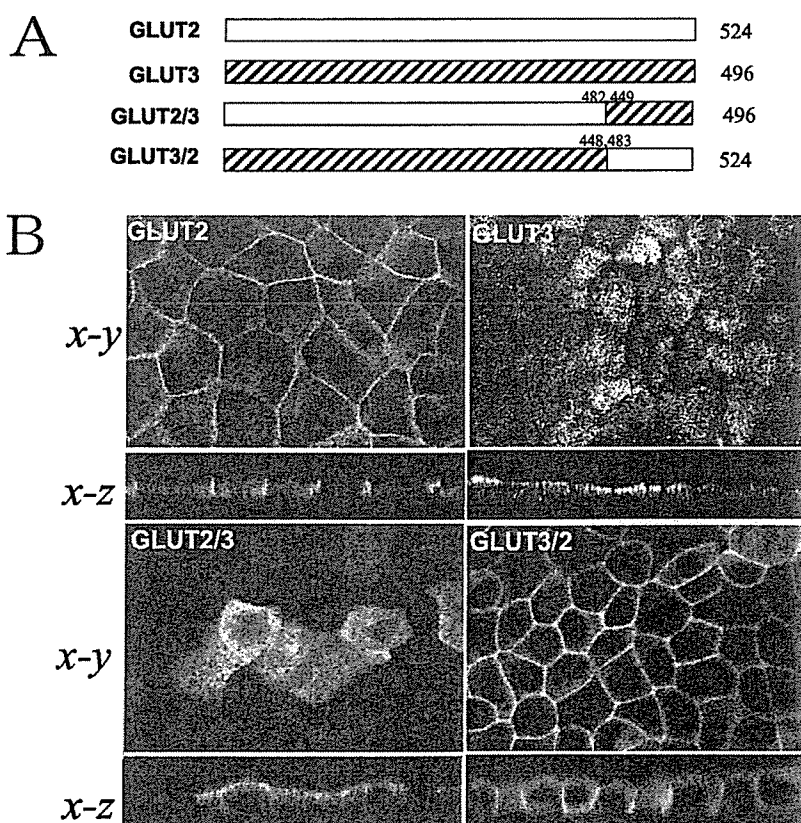


**Fig. 4.** Immunofluorescence Localizations of GLUT2, GLUT3, and Their Chimeric GLUTs

A, The GLUT2, GLUT3, and the two chimeras generated are represented in this *line drawing*. The chimeras consist of either GLUT2 or 3 up to and including the 12<sup>th</sup> transmembrane domain of each GLUT with the opposite C-terminal domain fused in frame, generating GLUT2/3 and GLUT3/2. B, At least 4 d before the immunofluorescence study depicted here, MDCK cells expressing the various proteins, as indicated, were plated onto coverslips. The proteins of interest were detected utilizing either an antibody raised against the C-terminal domain of GLUT2 (GLUT2 and GLUT3/2) or an antibody raised against the C-terminal domain of GLUT3 (GLUT3, GLUT2/3). Confocal images were collected and representative images are shown.

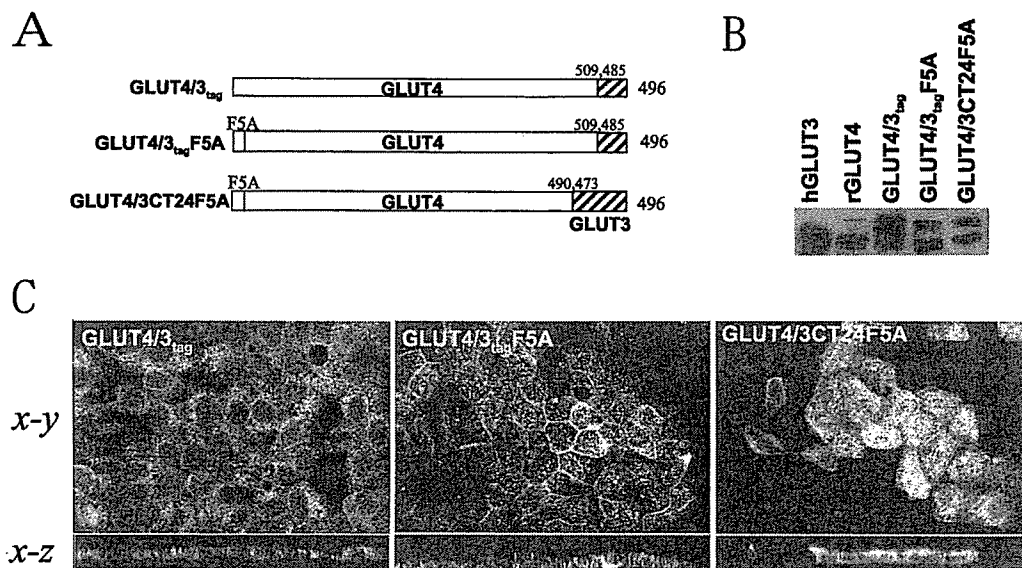


**Fig. 5.** Immunofluorescence Localizations of GLUT4 and GLUT4/3 Chimeric GLUTs

A, The cDNAs generated for this study and used to transfect MDCK cells are depicted here. As shown, all molecules bear the GLUT3 epitope tag at the extreme carboxy terminus with the Phe5 of GLUT4 mutated to Ala in both GLUT4/3<sub>tag</sub>F5A and GLUT4/3CT24F5A. B, Western blot analysis of total membrane samples prepared from MDCK cells. Recombinant GLUTs were detected with an anti-GLUT3 antibody. C, MDCK cells expressing GLUT4/3<sub>tag</sub>, GLUT4/3<sub>tag</sub>F5A, or GLUT4/3CT24F5A were plated at confluence and allowed to polarize over 5 d. The cellular localization of each of these proteins was assessed by confocal immunofluorescence microscopy using an antibody raised against the GLUT3 carboxy-terminal 12 residues. Representative images are presented.

cellular compartment (Fig. 5C, *middle panel*). Conversely, the chimera GLUT4/3CT24F5A composed of GLUT4 and the cytosolic C-terminal tail of GLUT3 and possessing the Phe5 to Ala mutation was targeted apically (Fig. 5C, *right panel*). Collectively, these data show that the GLUT3 tail possesses an apical targeting signal that does not include the C-terminal 12 a.a.

#### Further Analysis of GLUT1/3 Chimeras in MDCK Cells

To further define the composition of the apical targeting signal, we examined the targeting of a panel of GLUT1/3 chimeras comprising different portions of the C terminus of GLUT3. Consistent with the data described above (Fig. 5), a chimera in which the last seven a.a. of GLUT1 were replaced with the last 13 a.a. of hGLUT3 (GLUT1/3CT13) was targeted to the basolateral cell surface (Fig. 6C, *middle lower panel*). Intriguingly, addition of a further six a.a. from hGLUT3 (GLUT1/3CT19) resulted in a significant increase in apical targeting although some basolateral targeting was still evident (Fig. 6C, *left lower panel*). However, addition of a further five a.a. from GLUT3 to generate the chimera GLUT1/3CT24 resulted in predominantly apical targeting with little evidence of basolateral localization (Fig. 6C, *right upper panel*). To verify these data, we performed vectorial biotinylation as described above and found that GLUT1/3CT19 was targeted predominantly to the apical side whereas GLUT1/3CT13 was targeted primarily to the basolat-

eral side (Fig. 6D), consistent with our immunofluorescence studies.

As shown in Fig. 6C, expressed GLUT1 occasionally exhibits apparent apical staining in addition to the basolateral staining in immunohistochemical analysis. However, this does reflect, not mixed labeling to different surface domains, but rather both basolateral and intracellular labeling. When the GLUTs reside intracellularly, the outlines of cell nuclei can be seen clearly in x-y images. In contrast, when they localize in apical membranes, the outlines can barely be visualized. When GLUT1s are expressed (Fig. 6C, *left upper panel*), the staining pattern appears to be mixed, similar to those of GLUT1/5 (Fig. 3B) and GLUT3/2 (Fig. 4B). However, this expressed GLUT1 was proved to be located exclusively in the basolateral membrane by biotinylation experiments (Fig. 6D).

#### DISCUSSION

In the present study, we obtained evidence that the cytosolic carboxy-terminal tail of hGLUT3 contains a targeting motif capable of directing the trafficking of GLUTs 1, 2, and 4 to the apical cell surface in MDCK cells. By examining the targeting of a series of more defined GLUT1/3 chimeras, we found evidence for the presence of an apical targeting signal involving residues 473–484 (DRSGKDGVMEMN) in the carboxy tail. The finding of special interest is that chimeras con-



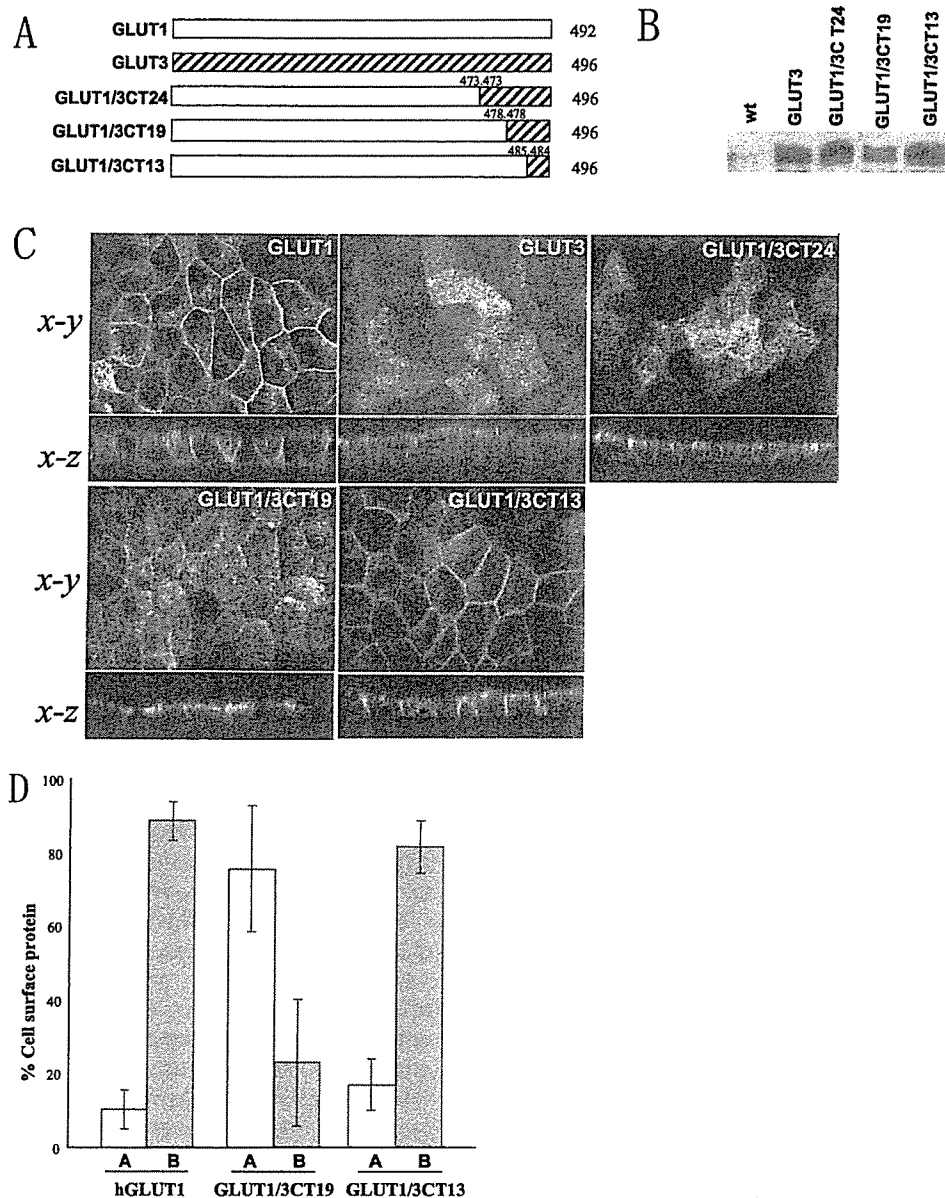


**Fig. 6.** Immunofluorescence Localizations of GLUT1, GLUT3, and Their Chimeric GLUTs

A, Stable MDCK cell lines were generated by transfection with cDNA, as depicted, and selection in G418. GLUT1/3CT24 consists of a.a. 1–473 of GLUT1 and a.a. 473–496 of GLUT3. Similarly, GLUT1/3CT19 and GLUT1/3CT13 were constructed by fusing a.a. 1–478 (CT19) or a.a. 1–485 (CT13) of GLUT1 to a.a. 478–496 (CT19) or a.a. 484–496 (CT13) of GLUT3. B, Membrane samples were prepared and subjected to SDS-PAGE and Western blot analysis to assess expression levels of GLUTs in MDCK cells. Membranes were incubated with an antibody raised against the C-terminal domain of GLUT3. C, MDCK cells were transfected (with cDNA as indicated in panel A) and clones were analyzed by immunofluorescence microscopy to ascertain the domain-specific localization of the recombinant transporters. Cells were fixed, permeabilized, and immunolabeled using an antibody raised against a short peptide derived from the intracellular loop of hGLUT1 (GLUT1) and an antibody raised against the C-terminal domain of GLUT3 (GLUT3, GLUT1/3CT24, GLUT1/3CT19, and GLUT1/3CT13). Confocal images were generated using a Zeiss Axiophot fluorescent microscope and a Bio-Rad MRC600 laser scanning head. D, Cell surface localizations of overexpressed hGLUT1, hGLUT1/3CT19, and hGLUT1/3CT13 were assessed using a domain-specific biotinylation assay. Cells were grown at confluence for 4–5 d on Transwell filters. Apical and basolateral cell surface proteins were biotinylated by addition of 0.5 mg/ml EZ-Link-Sulfo-NHS-Biotin (Pierce Chemical Co.) for 15 min. Biotinylated proteins were recovered and subjected to SDS-PAGE followed by Western blotting with antibodies specific for hGLUT1. Chemiluminescent bands were quantified using a Bio-Rad 600 densitometer, and signals detected were corrected to account for loading differences.

taining the last 12 or 13 a.a. of GLUT3 did not exhibit significant apical targeting, whereas a chimera containing a further seven a.a. from GLUT3 (GLUT1/

3CT19) exhibited significant apical targeting. Thus, fine mapping of the C-terminal tail of hGLUT3 has narrowed the apical sorting information to a small

region encompassing residues DGVMEMN, which corresponds to residues PAGVELN in rodent GLUT3. It is noteworthy that this chimera (GLUT1/3CT19) was partially targeted to the basolateral membrane whereas GLUT1/3CT24, which contained an additional five a.a. from GLUT3, was targeted almost indistinguishably from wild-type GLUT3. To our knowledge, no similar targeting motifs have been reported in other apical membrane proteins, and we have been unable to identify a similar motif in other apical membrane proteins. Most noteworthy is the presence of two conserved hydrophobic residues surrounding an acidic residue in both the rodent (VEL) and human (MEM) sequences. Future studies will be aimed at identifying the roles of these residues.

Based upon our initial studies with GLUT1/3 chimeras (Fig. 1), we hypothesized that the GLUT1 tail contained a basolateral signal that was disrupted in this chimera, resulting in default trafficking to the apical cell surface. However, detailed studies showed that this was not the case and argued in favor of an apical signal in GLUT3. Most notably, the GLUT3 tail facilitated apical targeting when grafted onto GLUT1, 2, or 4, all of which normally recycle via the basolateral cell surface. Thus far, two separate classes of basolateral sorting signals have been identified. These are characterized by either an essential tyrosine residue, or a dileucine motif (5–7). Similar kinds of motifs could not be found in the C termini of either GLUT1 or GLUT2 (Fig. 7). The LGA residues are conserved between GLUT1 and GLUT2 in the C terminus. However, mutating all of these residues did not disrupt the basolateral targeting of GLUT1 (data not shown). We also prepared a GLUT1 mutant missing the last three a.a. because this domain has been shown to act as a binding site for PDZ domain-containing proteins (29, 30). However, the distribution of this truncated GLUT1 was exactly the same as that of wild-type GLUT1 (data not shown). Thus, using this type of approach, we were unable to identify a basolateral targeting domain in the tail of GLUT1. Consistent with this conclusion, the GLUT1 tail did not significantly alter the apical targeting of a tail minus LDL-R, a construct that has been successfully used to map basolateral sorting signals in cytosolic tails (Fig. 2). Moreover, the cytosolic tail of GLUT5, which does not contain a basolat-

eral sorting signal, did not disrupt the targeting of GLUT1 (Fig. 3). Taken together, these studies provide compelling evidence that the C-terminal tail of GLUT3 contains an apical sorting signal. This signal is obviously very dominant, being able to overcome basolateral sorting signals in GLUTs 1, 2, and 4.

It was reported previously that some apical targeting motifs function by selectively partitioning into lipid raft domains in the Golgi (31). Intriguingly, it was reported recently that, in nonpolarized epithelial cells, whereas a substantial portion of GLUT1 was found in detergent-resistant membrane domains, this was not the case for GLUT3 (32). Hence, these data support the notion that GLUT3 is sorted via a non-lipid raft-mediated domain; this is consistent with the present data indicating such a domain to be located in the cytosol, perhaps allowing the transporter to interact with cytosolic targeting machinery. Several other reports have recently found narrowly defined sequences or short peptides in the C-terminal cytoplasmic tails of membrane proteins to have a role in apical targeting (33–37). Among them, multiple autonomous signals for apical targeting in the same protein have been reported (33, 34). These signals include PDZ-interacting domains (35) and  $\beta$ -turn structures (36) as well as less well-defined signals. Taken together, these observations suggest the apical sorting mechanism defined by cytosolic sorting signals to be less well defined than luminal or transmembrane signals, and further work is required to determine whether there is some type of homology among these motifs.

GLUT3 has been shown to undergo specialized targeting in other cell types. It is targeted to the limited membrane of secretory granules in platelets (38) and to the tail of sperm cells (39). Moreover, there is evidence that GLUT3 is targeted to axons in neurons (our unpublished data) and also to neuronal vesicles (40). It will be intriguing to determine whether the cytosolic C terminus is involved in each of these unique trafficking processes, which would imply a common mechanism. Consistent with this, it was previously suggested that similar rules govern the targeting of membrane proteins in epithelial cells and neurons (41).

The identification of this apical targeting signal in the GLUT3 tail may have significant utility in studying the structure/function of sugar transporters in mammalian

human	GLUT1-KVPETKGRTFDEIASGFRQGGASQSDKTPEEIFHPLGADSQV	492
human	GLUT2-KVPETKGSFEEIAAEFQKKSGSAHRPKAAVEMKFLGATETV	524
mouse	GLUT2-KVPETKGSFEEIAAEFRKKSGSAPPRKAAVQMEFLASSESV	523
human	GLUT3-KVPETGRRTFEDITRAFEGQAHGADRSGKD— <u>GVMEMNSIEPAKETTTNV</u>	496
mouse	GLUT3-KVPETKGRRTFEDIARAFEGQA— <u>SGKGPAGV-ELNSMQPVKETPGNA</u>	493
rat	GLUT3-KVPETKGRRTFEDITRAFEGQA— <u>SGKGSAGV-ELNSMQPVKETPGNA</u>	493
human	GLUT4-RVPETGRRTFDQISAAFHRTPSLLEQEVKPSLEYLGPDEND	509
human	GLUT5-IVPETKAKTFIEINQIFTKMKNVSEVYPEKEELKEL—PPVTSEQ	501
rat	GLUT5-VVPETKGRTFVEINQIFAKKNKVSVDVYPEKEE—KELNDLPPATREQ	502

Fig. 7. Comparison of the Cytosolic Tails of Human and Rodent GLUTs

The putative a.a. sequence, which is suggested to have an apical sorting signal, is *underlined*.

cells. A major complication of studying transport kinetics of GLUTs after their expression in mammalian cells is that there is always a very high background due to the presence of endogenous transporters. We previously found that glucose transport across the apical cell surface in MDCK cells is negligible because most of the uptake occurs via the basolateral surface (20). By transplanting the apical signal from GLUT3 onto other transporters it should be feasible to redirect them to the apical surface, as shown here, which should afford ideal conditions for studying transport kinetics in a more appropriate environment.

In conclusion, we have analyzed the asymmetric distribution of facilitative GLUTs by expressing chimeric transporters utilizing various portions of GLUTs (GLUT1–GLUT5) in MDCK cells. Our present data strongly suggest that the apical sorting signal resides in the C-terminal tail of GLUT3.

## MATERIALS AND METHODS

### cDNA Constructs

Chimeric cDNAs were produced according to previously described methods (42), which allowed us to swap different domains from different transporter isoforms at any desired junction. A hGLUT1 cDNA (23), a hGLUT2 cDNA (42), a hGLUT3 cDNA (27), a hGLUT4 cDNA (28), and a rat GLUT5 cDNA (43) were used as PCR templates. Cytomegalovirus-based expression plasmid pCB6 was generously supplied by Dr. Mellman (4). Fragments prepared by PCR were fully sequenced and observed to have no unexpected mutations. cDNAs encoding wild-type and chimeric GLUTs were ligated into pCB6 vectors.

### Cell Culture and Transfection

MDCK cells were cultured in DMEM supplemented with 10% fetal calf serum, 2 mM L-glutamine, 100 U/ml penicillin, and 100  $\mu$ g/ml streptomycin at 37 C, in 5% CO<sub>2</sub>. Lipofectamine reagent, Opti-MEM I, and G-418 (geneticin) were purchased from GIBCO Life Technologies (Eggenstein, Germany). One day before transfection, MDCK cells were trypsinized and seeded onto a 60-mm plastic culture dish at  $6 \times 10^5$  cells per dish. The following day, transfection procedures were performed using 30  $\mu$ l lipofectamine diluted in 300  $\mu$ l Opti-MEM I (supplemented with 20 mM L-glutamine) and 6  $\mu$ g GLUT/pCB6 diluted in 300  $\mu$ l of supplemental Opti-MEM-I/60-mm dish. Cells were incubated in the presence of the lipofectamine-DNA mix for 5 h at 37 C, in 5% CO<sub>2</sub>, and then incubated overnight in DMEM-10% fetal calf serum-L-glutamine. Forty-eight hours after transfection, each transfected 60-mm dish was split into three 150-mm dishes and incubated with G-418 (0.8 mg/ml). Colonies resistant to G-418 were isolated after 10–14 d and screened for protein expression by Western blotting.

### Western Blotting

To screen for positive expression of the chimera of interest, membrane protein samples (20  $\mu$ g protein) were subjected to SDS-PAGE employing a 10% resolving gel. Proteins were transferred to a nitrocellulose membrane. Membranes were incubated for 1 h at 37 C with the appropriate primary antibody. After three 10-min washes in PBS-0.1% Tween 20, the

membranes were incubated at room temperature for 1 h with a horseradish peroxidase-labeled donkey antirabbit secondary antibody (Amersham Life Science, Little Chalfont, Buckinghamshire, UK) diluted 1:10,000 in PBS-0.2% BSA. After three further washes, labeled proteins were visualized using the enhanced chemiluminescence detection method (Amersham Life Science).

### Preparation of Total Membrane Fractions

Total membrane fractions were prepared from MDCK cells after homogenization in 20 mM HEPES, pH 7.4, 1 mM EDTA, 255 mM sucrose buffer containing protease inhibitors (10  $\mu$ g/ml aprotinin, 10  $\mu$ g/ml leupeptin, 250  $\mu$ M phenylmethylsulfonyl fluoride) and centrifugation at 50,000 rpm in a Beckman TLA100-3 rotor (Beckman Coulter, Inc., Fullerton, CA) for 60 min. The membrane pellet was resuspended in 20 mM HEPES, pH 7.4, 1 mM EDTA, 255 mM sucrose buffer and stored at –80 C before use.

### Protein Assay

The protein concentration of total membrane fractions was determined using the bicinchoninic acid assay (Pierce Chemical Co., Rockford, IL) according to the manufacturer's instructions.

### Immunofluorescence Microscopy

Cells were plated at near-confluent density on glass coverslips and fixed 5 d later in 2% paraformaldehyde-PBS for 1 h at room temperature. Polarization was indicated by the presence of domes or blisters in the cultures. Coverslips were washed three times in PBS, and then quenched for 15 min in 0.2% Triton X-100. After an additional three washes in PBS, coverslips were blocked for 30 min in 2% horse serum-PBS and then washed twice in PBS. Primary antibodies were diluted in 0.1% horse serum-PBS, and incubations were carried out at 4 C overnight. Fluorescein isothiocyanate-conjugated antirabbit Ig secondary antibody diluted in 0.1% horse serum-PBS was applied after three 5-min washes in PBS. After a 1-h incubation, at room temperature, coverslips were washed three times in PBS for 5 min each and then mounted in 1% propyl gallate-50% glycerol-PBS. Confocal images were generated with a Zeiss Axiophot microscope (Carl Zeiss, Thornwood, NY) and a Bio-Rad MRC600 confocal laser scanning head (Bio-Rad Laboratories, Inc., Hercules, CA). At least one G-418-resistant clone, which was negative by immunoblotting, served as a negative control for immunofluorescence microscopy.

### Cell Surface Biotinylation

Localization of the LDL-R constructs and GLUT1/3 chimeras was assessed utilizing a domain-specific biotinylation assay. Briefly, MDCK cells expressing various chimeric proteins were plated onto transwell filters (Corning, Inc., Corning, NY) and grown for at least 4 d at 37 C and 5% CO<sub>2</sub>. To assess the integrity of the monolayer, growth media containing [<sup>14</sup>C]inulin (0.1 mCi/ml at 1:2000 dilution) were added to the apical chamber and incubated for 1 h. After this incubation, aliquots of medium from both the apical and basal chambers were counted (Coulter Counter, BD, Beckman Coulter, Inc.). Transwells with less than 0.5% transport were used in experiments. Filters were washed three times with ice-cold PBS containing 1 mM MgCl<sub>2</sub> and 0.1 mM CaCl<sub>2</sub> (PBS+). Apical or basal cell surfaces were incubated with 0.5 mg/ml EZ-link Sulfo-NHS-biotin (Pierce Chemical Co.) for 15 min on ice. This process was repeated, and the free biotin reagent was then quenched by washing with PBS+ containing 50 mM

glycine. Filters were transferred into lysis buffer (1% TX-100, 20 mM HEPES, 1 mM EDTA, 100 mM NaCl, aprotinin 10  $\mu$ g/ml, leupeptin 10  $\mu$ g/ml, and phenylmethylsulfonylfluoride 250  $\mu$ M) for 30 min on ice and vortexed, and solubilized material was cleared by centrifugation at 14,000 rpm at 4 C for 15 min. An aliquot of cleared supernatant served as the total expression sample, and the remainder was incubated with streptavidin-agarose (Sigma Chemical Co., St. Louis, MO) to recover biotinylated proteins. Immunoprecipitated proteins were subjected to SDS-PAGE and subsequent Western blot analysis using either a polyclonal LDL-R antibody, LB1 (gift from Dr. P. Kroon, Department of Biochemistry, University of Queensland), or antibodies specific to hGLUT1 (gift from Dr. G. Lienhard, Department of Biochemistry, Dartmouth Medical School, Hanover, NH). Detection was performed using goat antirabbit-horseradish peroxidase antibody (Amersham Life Science) and enhanced chemiluminescence (SuperSignal, Pierce Chemical Co.).

### Acknowledgments

Received March 18, 2003. Accepted October 30, 2003.

Address all correspondence and requests for reprints to: David E. James, Garvan Institute of Medical Research, St. Vincents Hospital, Sydney 2010, Australia. E-mail: d.james@garvan.org.au; or Yoshitomo Oka, Division of Molecular Metabolism and Diabetes, Department of Internal Medicine Tohoku University Graduate School of Medicine, Miyagi 980-8574, Japan. E-mail: oka@int3.med.tohoku.ac.jp.

K.I. and A.M.S. contributed equally to this work and should both be considered first authors.

This work was supported by the Research Council of Australia, of which D.E.J. is a Senior Principal Research Fellow of the National Health and Medical Research Council of Australia. This work was also supported by Grant-in Aid for Scientific Research no. 13470226 (to Y.O.) and Creative Basic Research Grant no. 10NP0201 (to Y.O.) from the Ministry of Education, Culture, Sports, Science, and Technology of Japan.

### REFERENCES

- Matter K, Mellman I 1994 Mechanisms of cell polarity: sorting and transport in epithelial cells. *Curr Opin Cell Biol* 6:545-554
- Simon K, Wandinger-Ness A 1990 Polarized sorting in epithelia. *Cell* 62:207-210
- Casanova JE, Apodaca G, Mostov KE 1991 An autonomous signal for basolateral sorting in the cytoplasmic domain of the polymeric immunoglobulin receptor. *Cell* 66:65-75
- Hunziker W, Harter C, Matter K, Mellman I 1991 Basolateral sorting in MDCK cells requires a distinct cytoplasmic domain determinant. *Cell* 66:907-920
- Marks MS, Ohno H, Kirchhausen T, Bonifacino JS 1997 Protein sorting by tyrosine-based signals: adapting to the Ys and wherefore. *Trends Cell Biol* 7:124-128
- Pond L, Kuhn LA, Teyton L, Schutze MP, Tainer JA, Jackson MR, Peterson PA 1995 A role for acidic residues in di-leucine motif-based targeting to the endocytic pathway. *J Biol Chem* 270:19989-19997
- Sandoval IV, Bakke O 1994 Targeting of membrane proteins to endosomes and lysosomes. *Trends Cell Biol* 4:292-297
- Rapoport I, Chen YC, Cupers P, Shoelson S, Kirchhausen T 1998 Dileucine-based sorting signals bind to the  $\beta$  chain of AP-1 at a site distinct and regulated differently from the tyrosine-based motif-binding site. *EMBO J* 17:2148-2155
- Rapoport I, Moyazaki M, Boll W, Duckworth B, Cantley LC, Shoelson S, Kirchhausen T 1997 Regulatory interactions in the recognition of tyrosine-based endocytic signals by clathrin AP-2 complexes. *EMBO J* 16:2240-2250
- Rodionov DG, Bakke O 1998 Medium chains of adaptor complexes AP-1 and AP-2 recognize leucine-based sorting signals from the invariant chain. *J Biol Chem* 273:6005-6008
- Urban J, Parczyk K, Leutz A, Kayne M, Kondor-Koch C 1987 Constitutive apical secretion of an 80-kD sulfated glycoprotein complex in the polarized epithelial Madin-Darby canine kidney cell line. *J Cell Biol* 105:2735-2743
- Kitagawa Y, Sano Y, Ueda M, Higashio K, Narita H, Okano M, Matsumoto S, Sasaki R 1994 N-glycosylation of erythropoietin is critical for apical secretion by Madin-Darby canine kidney cells. *Exp Cell Res* 213:449-457
- Jacob R, Alfalah M, Grunberg J, Obendorf M, Naim HY 2000 Structural determinants required for apical sorting of an intestinal brush-border membrane protein. *J Biol Chem* 275:6566-6572
- Monlauzeur L, Breuza L, Le Bivic A 1998 Putative O-glycosylation sites and a membrane anchor are necessary for apical delivery of the human neurotrophin receptor in Caco-2 cells. *J Biol Chem* 273:30263-30270
- Bell GI, Kayano T, Buse JB, Burant CF, Takeda J, Lin D, Fukumoto H, Seino S 1990 Molecular biology of mammalian glucose transporter. *Diabetes Care* 13:198-208
- Thorens B, Cheng ZQ, Brown D, Lodish HF 1990 Liver glucose transporter: a basolateral protein in hepatocytes and intestine and kidney cells. *Am J Physiol* 259:C279-C285
- Rand EB, Depaoli AM, Davidson NO, Bell GI, Burant CF 1993 Sequence, tissue distribution, and functional characterization of the rat fructose transporter GLUT5. *Am J Physiol* 264:G1169-G1176
- Harris DS, Slot JW, Geuze HJ, James DE 1992 Polarized distribution of glucose transporter isoforms in Caco-2 cells. *Proc Natl Acad Sci USA* 89:7556-7560
- Davidson NO, Hausman AML, Ifkovits CA, Buse JB, Gould GW, Burant CF, Bell GI 1992 Human intestinal glucose transporter expression and localization of GLUT5. *Am J Physiol* 262:C795-C800
- Pascoe WS, Inukai K, Oka Y, Slot JW, James DE 1996 Differential targeting of facilitative glucose transporter in polarized epithelial cells. *Am J Physiol* 271:C547-C554
- Inukai K, Katagiri H, Takata K, Asano T, Anai M, Ishihara H, Nakazaki M, Kikuchi M, Yazaki Y, Oka Y 1995 Characterization of rat GLUT5 and functional analysis of chimeric proteins of GLUT1 glucose transporter and GLUT5 fructose transporter. *Endocrinology* 136:4850-4857
- Colville CA, Seatter MJ, Jess TJ, Gould GW, Thomas HM 1993 Kinetic analysis of the liver-type (GLUT2) and brain-type (GLUT3) glucose transporter in *Xenopus* oocytes: substrates specificities and effects of transport inhibitors. *Biochem J* 290:701-706
- Davies A, Ciardelli TL, Lienhard GE, Boyle JM, Whetton AD, Baldwin SA 1990 Site-specific antibodies as probes of the topology and function of the human erythrocyte glucose transporter. *Biochem J* 266:799-808
- Matter K, Hunziker W, Mellman I 1992 The cytoplasmic domain contains two tyrosine-dependent targeting determinants. *Cell* 71:741-753
- Matter K, Whitney JA, Yamamoto EM, Mellman I 1993 Common signals control low density lipoprotein receptor sorting in endosomes and the Golgi complex of MDCK cells. *Cell* 74:1053-1064
- Inukai K, Takata K, Asano T, Katagiri H, Ishihara H, Nakazaki M, Fukushima Y, Yazaki Y, Kikuchi M, Oka Y 1997 Targeting of GLUT1-GLUT5 chimeric proteins in the polarized cell line Caco-2. *Mol Endocrinol* 11:442-449
- Shewan AM, Marsh BJ, Melvin DR, Martin S, Gould GW, James DE 2000 The cytosolic C-terminus of the glucose transporter GLUT4 contains an acidic cluster endosomal